INTERNATIONAL ATOMIC ENERGY AGENCY
UNITED NATIONS EDUCATIONAL, SCIENTIFIC AND CULTURAL ORGANIZATION

INTERNATIONAL CENTRE FOR THEORETICAL PHYSICS
34100 TRIESTE (ITALY) - P.O.B. 586 - MIRAMARE - STRADA COSTIERA 11 - TELEPHONES: 224281/2/3/4/5/6
CABLE: CENTRATOM - TELEX 460392-1

SMR/110/A - 9

WORKING PARTY

ON

"PHYSICS OF CONDENSED MATTER AT PLANETARY PRESSURES"

(20 August - 7 September 1984)

PROPERTIES OF IRON AT THE EARTH'S CORE CONDITIONS

O.L. ANDERSON

Department of Earth and Space Sciences

University of California, Los Angeles
3806 Geology Building
Los Angeles, California 90024, USA

Properties of Iron at the Earth's Core Conditions

A. The Composition of the Core.

Although the composition of the inner core has long been debated, the consensus now heavily favors an iron core where the inner core is very nearly pure iron, and the outer core is a mixture of iron and some solute. Birch (1952) argued that iron is alloyed with some lighter element, especially in the outer core, strictly on density grounds. Since that time, although the nature and distribution of the alloying element(s) has been a matter of contention, there is good agreement that in the core, the major element is iron.

The cosmological argument in favor of a predominantly iron core relies on the assumption of homogeneity in the solar system insofar as element distribution is concerned. If the element distribution is to be maintained, the number of Fe atoms should be close to the number of Si atoms in the Earth (Ross and Aller, 1976; Ganapathy and Anders, 1974; Wasson, 1984). Since iron is depleted relative to Si in the Earth's mantle, it needs to be greatly enriched in the Earth's core. The volume of the mantle is much greater than the core. Consequently, the core has to be composed essentially all of iron, to maintain the cosmic abundance ratio.

Experimental geophysics has provided a great deal of data which support the model of an iron core. The most important experimental evidence is from shock-wave physics. The shock-wave evidence will now be reviewed.

Birch (1963), in analyzing the then existent shock-wave data on metals, especially the data from the Los Alamos Scientific Laboratory, noticed that there was a definite relation between the bulk sound velocity, $\varphi = \sqrt{K/\rho} = (V_P^2 - 4/3V_S^2)^{1/2}$ and ρ. K is the bulk modulus and ρ is density, and V_P and V_S are the longitudinal and shear sound velocities. This relation, however, depends upon the atomic number. For metals up to atomic number 50, the higher the atomic number, the lower the value of φ for the same density. This is shown in Figure 1.

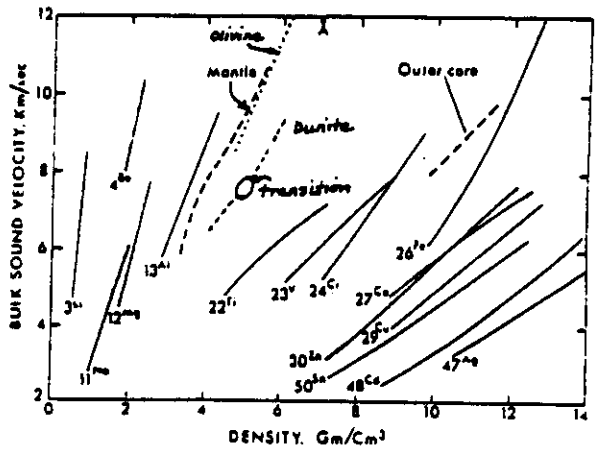

Figure 1. Relationship between φ and ρ for metals, showing the dependence on atomic number (McQueen and Marsh, 1960). The data for the Earth's mantle, the outer core, and olivine and dunite are shown for comparison. The dot-dash line is for a dunite rock with a midpoint transition of 5.5 gm/cm^3 (McQueen, et al., 1967), and A is the point for dunite at 6.8 gm/cm^3 (Altschuler and Kormer, 1961).

The data for dunite, Figure 1, illustrates the typical situation for phase changes on a velocity-density plot. A phase change merely extends the curve along the projection of the lower phase curve. This rule is the result of investigations that have come to be called velocity-density systematics (Anderson, 1966; Anderson and Anderson, 1970; Shankland, 1972; and Davies, 1974). All the oxides and silicate minerals lie in the domain of atomic number 13-15, shown in Figure 1.

It appears that a silicate, compressed to the densities found in the core, should have a sound velocity, φ, in excess of 20 km/sec. Thus, the bulk sound velocity of the core, derived from seismology, is much too low to arise from a silicate. Further, the core, whatever it is, should be composed of elements whose average atomic number is in the 25-27 range.

This correlation, described by Birch, convinced most researchers that the Earth's core was predominantly iron. Attention shifted to the properties of iron, and the chief experiments used shock-wave techniques on iron and iron alloys.

The fundamental experimental curve from shock waves is the Hugoniot, which is a description of how the temperature varies with pressure, when energy, momentum, and mass are conserved across a boundary of contact. The Hugoniot is neither isothermal or adiabatic, and to get the isotherm or the adiabat from it requires transformations involving the Grüneisen parameter.

The Hugoniot of iron is plotted below in Figure 2.

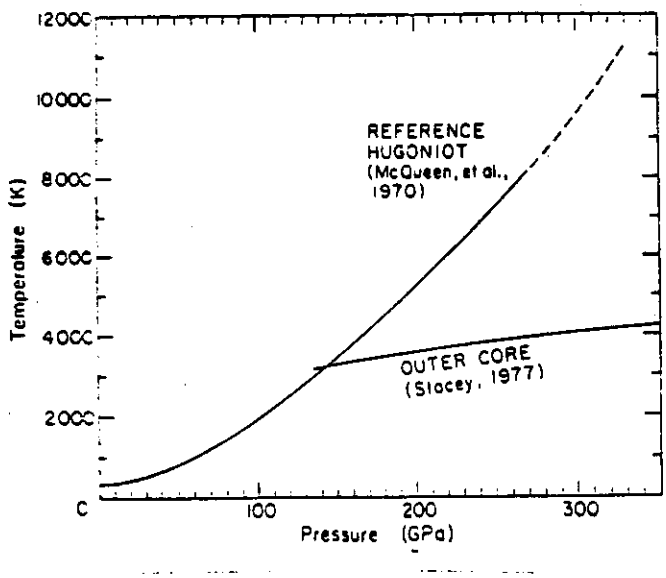

Figure 2. The Hugoniot of iron, compared to the temperature profile of the outer core computed by Stacey.

Since the outer core is liquid, we see that the upper portion of the Hugoniot is in the liquid state, while the lower part is in the solid state. The Hugoniot is insensitive to transitions.

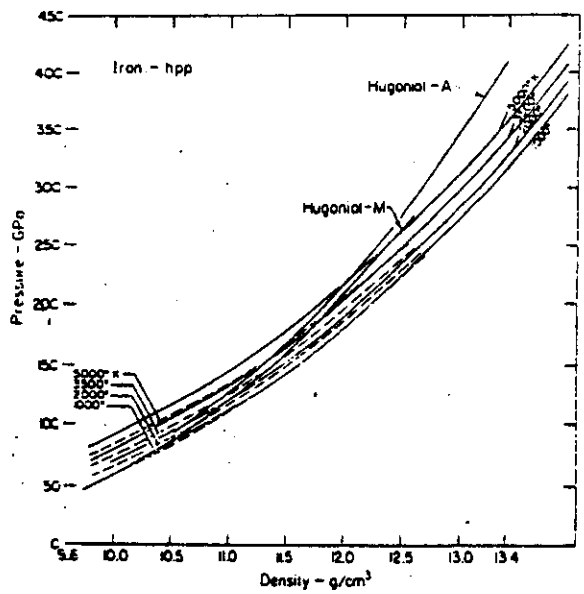

Figure 3. The isotherms of pure iron computed from the Hugoniot, assuming a hexagonal close packed structure (Ahrens, 1980).

Now, the corrections for the Hugoniot to the isotherms can be calculated. Ahrens (1980) did this calculation for a particular phase of iron (the hexagonal closely packed or ε-phase).

Assuming we know something about the temperature structure of the core (as in the Stacey 1977 model), the pressure density curves can be calculated along a geotherm of the core. This is shown below in Figure 4, and compared with seismic data.

Note that the data on pure iron is shifted to the right of the seismic data (noted by 1066A, QM3, Hart, et al., 1977).

On the other hand, the shock wave data on alloys of Fe, such as for FeS_2, shift it to the left of the seismic data.

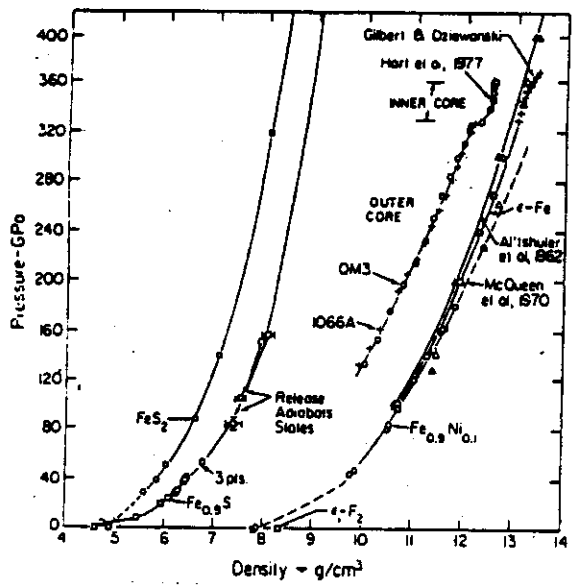

Figure 4. Compression curves along the geotherm, for Fe, as compared to seismic data (Ahrens, 1979).

Note that the pure iron data is close to the inner core seismic data. In fact, it coincides for the CAL 6 model (not shown in Figure 4) (Bolt and Urhammer, 1982).

Obviously, mixtures of iron and some other elements can be made so that the resulting Hugoniots coincide exactly with the seismic data of the outer core. Three candidates are carbon, sulfur, and oxygen. Mixing the shock wave data, as shown in Figure 4, requires 11% weight carbon, or 10-13% weight sulfur, or 7-8% weight oxygen. This is shown in Table 1.

Table 1. Candidate Light Element of the Earth's Core and Cosmochemical Abundances

Light Element (X) in the Core	Reuss Mixtures	Wt., % Core	(X/Si) Atomic Fraction, Earth	(X/Si) Atomic Fraction, Chrondritic Abundance*	(X/Si) Atomic Fraction, Solar Abundance †
C	Fe + C	11	0.44-0.63	0.006	5.9-14.5
S 0.24-0.52	$Fe_{0.9}S$ + Fe		10-13	0.14-0.29	0.11
	also FeS_2 + Fe	9-13			
O	$Fe_{0.94}O$ + Fe	7-8	3-4	3.5	13.8-21.4

*Ganapathy & Anders (1974)
†Ross & Aller (1976)

The cosmic abundance of sulfur agrees with the shock wave solution for sulfur, but there is not very good agreement for carbon. A reasonable case can be made for oxygen.

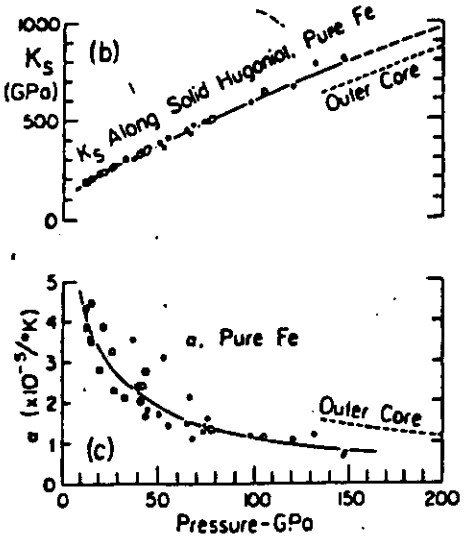

Figure 5. The shock wave solution for bulk modulus and thermal expansivity for pure iron compared to the outer core (after Jeanloz, 1979)

A number of physical properties of shocked iron can be compared with the core. In Figures 5 and 6 we see Jeanloz's (1979) solution for the bulk modulus and thermal

expansivity compared to the outer core. The outer core needs a smaller K_S and a larger α than in pure iron. As shown in Figure 6, the value for the bulk modulus of pure iron tends to extrapolate directly in the values for the inner core.

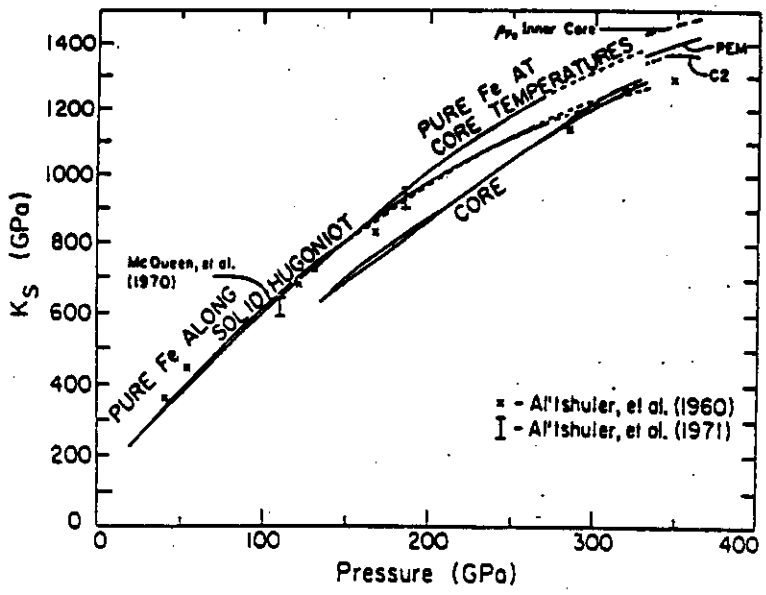

Figure 6. K_S of pure iron vs P, for pure iron and the Earth's core (Jeanloz, 1979).

Even better agreement is found for the comparison of the bulk sound velocity of pure iron with the core as shown in Figure 7.

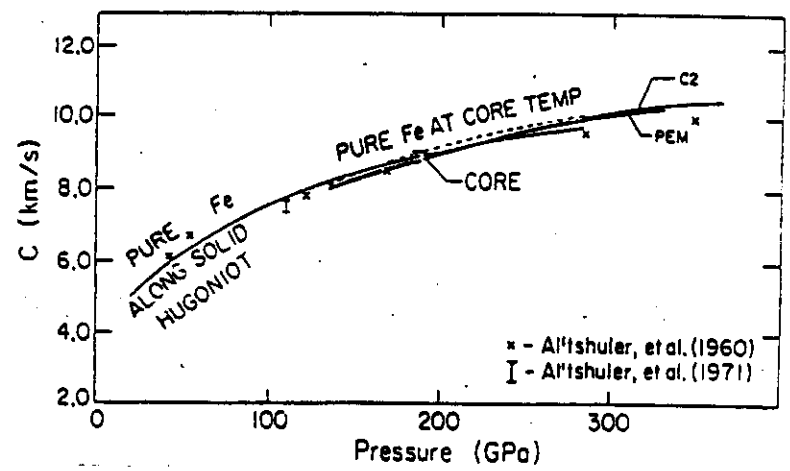

Figure 7. The bulk sound velocity, C, for pure iron and for the Earth's core (Jeanloz, 1979).

The assertion that the inner core has the properties of pure iron contrasts with previous opinions that the inner core has the properties of iron-nickel compounds (McQueen and Marsh, 1966; Birch, 1952; Brett, 1976; Al'tschuler, et al., 1968).

The alternative to the iron core model is to assume, as was done by Lyttleton (1963, 1965) and by Ramsey (1949, 1950), that the core is a metallized form of the mantle ionized under pressure. Experimental geophysics is now capable of observing any phase change that would transform an oxide into a metallic conductor at core pressures. Phase changes in oxides exist at high pressure, but the density change is small compared to that required for the mantle-core boundary of the Earth. From Figure 1, we see that a silicate most probably cannot duplicate the velocity of the core.

One report has been made, (Pavloskii, et al., 1977) in which a large density change for SiO_2 has been observed. An isentropic compression with a superstrong magnetic field (at about 150 GPa) apparently yielded a density corresponding to core conditions. This anamolous result is inconsistent with all other shock-wave experiments on SiO_2, and needs experimental confirmation. No such shock wave densification of α-quartz has been observed. Trunin, et al. (1971), concluded that no discontinuities exist in quartz above the stishovite transition even up to 650 GPa.

B. <u>The Phase Diagram of Pure Iron at Low Pressure</u>.

The iron we are most familiar with in everyday life is the α-phase, with a body centered cubic structure. This is certainly not the phase of iron that is in the Earth's core. The phase in the core is either the ε-phase (hexagonal closed packed) or γ (face centered cubic), but the evidence is in favor of the ε-phase as we shall see. There is also a high temperature-low pressure phase, δ, which like α, is body-centered cubic. The phase diagram is well measured up to 20 GPa and 2000° C. We see that in this region and above 5.2 GPa, liquid iron is in equilibrium with the γ-phase. The γ-liquid phase boundary is well measured up to 20GPa (Bundy, 1965). There are four solid phases and one liquid phase, so we have three triple points (t.p.). The γ-δ-ℓ triple point is at 1970 K and 5.2 GPa, and must be the beginning point of any extrapolation of the iron solidus into core pressures and temperatures. The α-ε-γ triple point is at 750° K and 11 GPa (Bundy, 1965). The slope

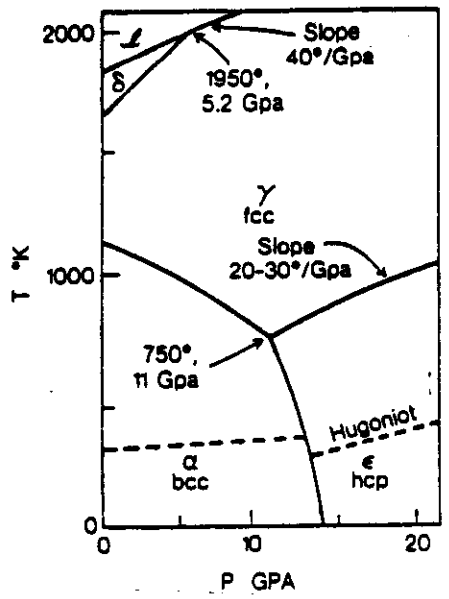

Figure 8. The low pressure phase diagram of iron (Liu, 1975).

boundary between the ε and γ phases has been in dispute. Bundy's (1965) measured value is 28°/GPa. The slope at the triple point must be in accordance with the boundary conditions at a t.p. (e.g., the sums of the volume changes, and the sum of the entropy changes is zero). Since $(\Delta S/\Delta V) = \Delta P/\Delta T$, then $\Delta P/\Delta T$ at the γ-ε boundary can be found if two other slopes, $\Delta P/\Delta T$, are known and the three volume changes around the t.p. are known. On this basis, Liu (1975) estimated dT/dP for the ε-γ boundary to be 31°/GPa. An earlier estimate by Takahashi and Bassett (1964) gave dT/dP = 20°/GPa. The total evidence suggests dT/dP for the ε-γ equilibrium is between 20 and 30°/GPa near the α-ε-γ triple point (but probably closer to the upper value).

The triple point (ε-γ-α) occurs somewhere at high pressure, and the absence of direct experimental information limits our knowledge of the structure of iron at inner-core pressures. If the t.p. occurs at pressure less than 320 GPa, then the inner core is in the ε-iron field. If the t.p. is greater than 350 GPa, then the inner core is in the γ-iron field. Liu (1975) showed that a straight extrapolation of the slope 30°/GPa would place the triple point somewhere around 93.5 GPa, in which case the inner core is ε-iron. As we shall see below, this straight line extrapolation (30°/GPa) is not justified. Nevertheless, we shall conclude that the inner core is in the ε-phase field.

There is no guarantee that dT/dP is invarient with pressure. If this were so, then the ΔS would diminish at the same rate as ΔV. That is not the case for the alkali halides, where ΔS decreases as $(\Delta V)V$, or $\Delta T/\Delta P \propto V$ (Jeanloz, 1982).

The measurement of the volume change between α and γ (1184° K and 0 P) shows a small negative change (-0.075 cm^3/mole) Birch (1972) (e.g., a slight increase in ρ_o). The volume change between α and ε (at 300° K and 13 GPa) shows a substantial decrease in volume (-0.389 cm^3/mole) (e.g., a large increase in ρ_o).

C. Equation of State Parameters for Iron.

Taking the volume of the α-phase at 1184° and 0 P to be 7.09 cc/mole, the volume of the γ phase at 1184° and 0 pressure is V_γ = 7.09 - 0.075 = 7.016 cm^3/mole. The density of the γ phase at 1184° (0 P) is thus ρ_γ = (55.83)/7.016 = 7.95 gm/cm^3. Taking the expansivity to be 7 x 10^{-6} over a temperature range of (300°-1184°), we estimate the density of the γ phase to be about 8.00 gm/cm^3 at room temperature and 0 pressure. Thus, on the basis of experiments and thermodynamic data, the room temperature values of the EOS parameters which are known for the three phases are shown in Table 2.

Table 2. Equation of State Parameters for Phases of Iron. Room Temperature Pressures

Iron Phase (P=0, T=300°K)	ρ_o	K_o GPa	K_o'	Source
α	7.873	166.6	5.29	Guinan and Beshers (1968)
	7.873	166.6	5.97	Rotter and Smith (1966)
ε	8.28	178.2	5.15	Reduced shockwave data (Brown & McQueen, 1982)
ε	8.28	156.2	5.4	Static compression. Murnaghan EOS (Mao and Bell, 1979)
ε	8.38	182.7		Andrews, 1973
γ	8.0	?	?	
(liquid iron at 1950°K)	(7.0)	(136.0)	(5.0)	Phase diagram and sound velocity (Birch, 1972; Filipov, et al., 1966)

The properties of α-iron can be considered secure because this phase is well measured. For ε-iron, the value found by Mao and Bell (1979) for K_o is suspiciously small, because it is smaller than K_o for α-iron. K_o ordinarily increases between phases in proportion to density increase so K_o for ε should be

greater than 166 GPa. The Mao and Bell result for K_o' may have arisen because they constrained their data to fit a Murnaghan EOS, which is not appropriate up to their limit (100 GPa). Thus, $K_o = 178$ GPa is probably the best value for ε-iron. The shock wave determined value of K_o may be influenced by the very high temperatures found in the upper ranges of the ε field. A better figure might be $K_o' = 5.5 \pm 0.5$.

This table shows that the properties of γ-iron should be between the α- and ε-phases. They may be closer to that of the well understood α-iron, than to the properties of ε-iron.

It becomes of some importance, therefore, to decide which of the two phases (γ or ε) are stable at core conditions. Fortunately, a new set of experiments in shock wave physics has helped clarify this issue.

D. The Measurement of Sound Velocity, V_P, in Highly Compressed Iron.

Most shock wave analyses arise from experiments which measure the shock velocity vs particle velocity.

$$U_S = \varphi_o + sU_P \qquad (1)$$

where φ_o is the bulk sound velocity

$$(\varphi_o = \sqrt{K_o/\rho_o}) \qquad (2)$$

at ambient conditions and s is the inferred slope. From this data, the Hugoniot is calculated. The shock velocity is the primary measured variable, and all properties determined are in P-V-T space. Because the bulk velocity is insensitive to phase transitions and the crossing of the solid-liquid interface, the Hugoniot sometimes does not give clues to phase boundaries. Such is the case for iron. Nothing about the Hugoniot in Figure 2 is suggestive of a liquid-solid boundary, although one must exist along the Hugoniot.

Although the bulk sound velocity is insensitive to a solid liquid transition, the sound velocities, V_P and V_S, are quite sensitive to such a transition, because V_S vanishes in the liquid state. A measurement of V_P near the liquid-solid phase boundary has the following properties: V_P is greater than the bulk sound velocity in the solid, but equal to the bulk sound velocity in the liquid. At the transition point, V_P slows from a compressional wave to a lower value representing the bulk wave velocity.

A recent innovation in shock wave techniques has permitted, for the first time, a good measurement of V_P in shocked iron (Brown and McQueen, 1980, 1982). The essential physics of this technique lies in the fact that a bulk wave is transformed at a boundary into two reflected waves, one of which is a compressional wave with velocity, V_P. Since V_P is faster than φ, V_P is propagated for a short time in the material under the highest compression. The experiment consists of isolating the transit time of the compressional wave in this state, and finding the corresponding pressure.

Now the Hugoniot is known to rise within the ε-phase. Up until the Brown and McQueen experiment, it was not known whether the Hugoniot crossed into the γ-phase before the liquid state was reached. Brown and McQueen (1982) found the ε-γ boundary was reached at 200 ± 2GPa, with a temperature of 4400 ± 300 K. They found that the pressure where V_P converged to φ to be 250 GPa ± 10 GPa (later revised downward to 243 ± 2; (Brown and McQueen, 1984)). From the Hugoniot data, they first estimated the liquid transition to be between 5000° K and 6000° K. A plot of their fundamental curve (V_P vs pressure) is given in Figure 9.

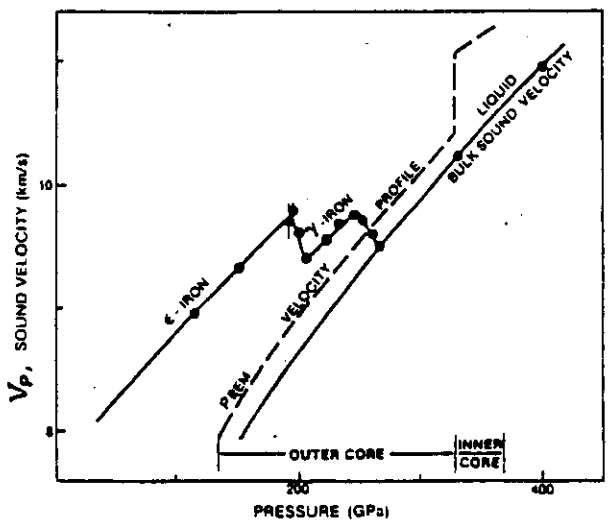

Figure 9. Sound velocity, V_P vs pressure for pure iron (Brown and McQueen, 1982, 1984). The first peak is at the ε-γ-iron transition, and the second peak is at the γ-liquid transition. PREM refers to the velocity profile of the Dzewonski and Anderson (1981) model.

We see that ε-iron has the higher velocity, indicating that γ-iron has a Poisson ratio closer to that of the liquid. This is reasonable since γ-iron is

the higher temperature phase (see Figure 8). Note that V_P of ε-iron extrapolates into the PREM values of V_P for the inner core (Dziewonski and Anderson, 1981). This is another bit of evidence that the inner core is essentially pure iron.

We see from Figure 9 that the PREM velocity profile of the outer core lies substantially below both ε-iron and γ-iron, thus suggesting that the outer core is not pure iron. The joining of the experimental points with the bulk sound velocity indicates the pressure where the Hugoniot crosses the γ-liquid boundary.

Anderson (1982) passed a Lindemann-type melting curve, as modified by Stevenson (1980), from the γ-δ-ℓ triple point at 5.2 GPa through the measured liquid transition, measured by shock waves, at 250 GPa (Brown and McQueen, 1982, 1984). This Lindemann curve was then additionally extrapolated from 250 GPa to the inner-outer core boundary pressure of 330 GPa, obtaining the temperature limits of the liquid-solid phase to be 5200-6600° K. Later Brown and McQueen (1984), using their additional experimental data, re-estimated the temperature at the inner-outer core boundary, finding 5800° K ± 500° K.

Additional analysis of the data behind Figure 9 provides further evidence that the inner core is pure ε-iron. From the bulk velocity and the compressional velocity, Poisson's ratio is estimated (Figure 10).

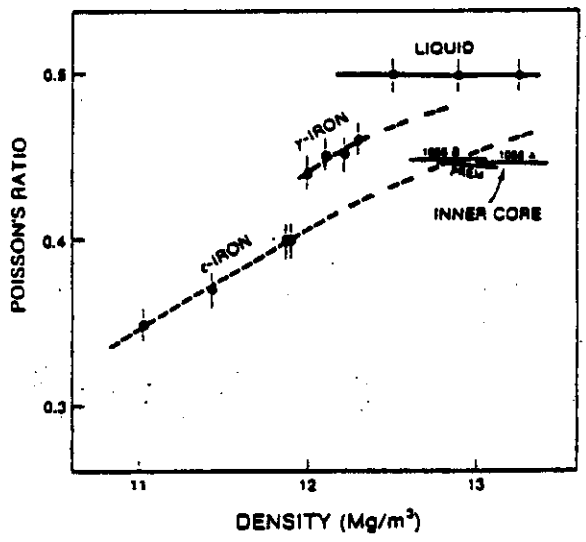

Figure 10. Poisson's ratio, σ, vs density for shocked iron. Note that the ε-iron data for σ extrapolates into the inner core data. PREM data is from Dziewonski and Anderson (1981); 1066B and 1066A data are from Gilbert and Dziewonski (1975).

E. The Melting Temperature of Iron of High Pressure.

As emphasized by Verhoogen (1980) and Stevenson (1980), a theory of melting should not rest exclusively on a solid state theoretical basis. For this reason, the Lindemann law has been criticized when used for melting curves extrapolated to high pressure. The Lindemann law (1910), written in its differential form, is

$$\frac{1}{T_m}\frac{dT_m}{dP} = \frac{2}{K_m}(\gamma - \tfrac{1}{3}) \qquad (3)$$

where γ is the Grüneisen parameter, T_m is the melting temperature, and K_m is the bulk modulus at melting. The original derivation was based on simplified lattice theory.

However, there have been at least two recent theoretical papers which show that a more fundamental approach accounting for the liquid state yields the same Lindemann equation, with small variations.

Stevenson (1980) derived two equations from liquid theory, valid at high P and near T_m that are important to the calculation of the melting curve.

$$dK/dP = 5 - 5.6\ P/K \qquad (4)$$

(which neglects a small term due to thermal energy), and

$$\frac{1}{T_m}\frac{dT_m}{dP} = \frac{1}{K_m}\frac{2(C_V^{vib}\gamma - R)}{(2C_V^{vib} - 3R)} \qquad (5)$$

where C_V^{vib} is the lattice vibrational contribution to the heat capacity, γ is the thermodynamic Grüneisen ratio, and R is the gas constant. Neither C_V^{vib} nor γ include electronic corrections.

Equation (5) is the liquid state equivalent of Lindemann's law, and reduces to it exactly within the classical limit $C_V^{vib} = 3R$. Grover (1971) has shown that in general C_V^{vib} is not equal to 3R for T_m for liquid metals. He showed that C_V^{vib} for several metals has a wide cusp at T_m, in which the specific heat rises substantially above 3R. Such a cusp is consistent with an order-disorder transformation. Values of the parameter C_V^{vib} for metals vary between 3.3R and 3.9R at low pressures.

Equation (3), as developed by Lindemann, does not satisfy the criteria that a melting theory should be based upon equilibrium between the liquid and the solid state.

Stacey and Irvine (1977) derived an equation analogous to (3) by using a thermodynamic theory starting from the Clausius-Clapeyron equation. They found:

$$\frac{1}{T_m}\frac{dT_m}{dP} = \frac{1}{K_m}\left[2(\gamma - 2\gamma^2\varepsilon)\right] \qquad (6)$$

The term containing ε arises from a thermal expansivity correction, $\varepsilon = \alpha T_m$, and will be a small percentage of γ. Equations (5) and (6) thus answer the objection of many that Lindemann's law is based only upon properties of the solid state.

Anderson (1982) used (5), and the value $C_V^{vib} = 3.5R$, to compute the melting curve between γ-iron and the liquid from 5.2 GPa up to 330 GPa, and Spiliopoulos and Stacey (1984) used (3) to compute the ε-iron-liquid melting curve between 250 and 330 GPa.

The differences between (6) and (3), and between (5) and (3) are not significant in view of the uncertainties in the extrapolated values of K_m and γ. Thus, Equation (3) will be used (as was done by Spiliopoulos and Stacey (1984)) as an approximation to the liquid state theoretical equation, and as an approximation to the theoretical equation derived from equilibrium (between liquid and solid) theory.

The approach used in this section is as follows:

1. The thermodynamic data at the lower end of the γ-ℓ boundary (5.2 GPa) will be used to evaluate the parameter γ in (3).

2. The equation relating volume compression and melting temperature will be found.

3. The equation will be integrated to obtain T_m vs ρ_o/ρ, where ρ_o refers to the density at 5.2 GPa and 1950°K (the ρ-γ-ℓ triple point).

4. The ratio of the volume at 5.2 GPa and 1950°K to the volume of iron at standard pressure and temperature will be found.

5. The value of T_m and the pressure along the γ-phase liquid boundary will be found, relative to the density of the solid.

In this approach, the extrapolation is made outwards in pressure from accurately known data at lower pressure. One parameter, $\gamma = d\ell n\gamma/d\ell n\rho$, is tuned so that the T_m trajectory intersects the data provided by the shock wave data at 243 GPa. As a consequence, both the low pressure data and the high pressure data are satisfied by equations developed from the Lindemann formula.

The constants in (3) must now be evaluated as a function of P. The density of liquid iron at P = 0 is 7.00 g cm^{-3} at 1868 K. The velocity of sound in liquid iron at atmospheric pressure is 4.4 km s^{-1} according to Filipov, et al. (1966) (a smaller value is given by Kurz and Lux (1969)). This value, coupled with the density, gives K_0 = 136 GPa, at 1868°K.

It is important to determine the value of γ at the initial integration point (5.2 GPa and 1970°K) which is the (δ-γ-ℓ) triple point. We have $T_m(5.2)$ = 1970 (Birch, 1972) and thus K(5.2) = 165. Further, dT/dP(5.2) = 38.5°/GPa (Strong, et al., 1963).

Using (3)

$$\gamma(5.2) = 1/3 + 1/2\ (K_m/T_m)\ (dT_m/dP) \qquad (7)$$
$$= 1.95$$

We shall compute the compression along the γ-liquid fusion curve, starting from the δ-γ-ℓ triple point (5.2 GPa). Anticipating the result that the ε-γ-ℓ triple point shall be in the vicinity of 280 GPa, as shown in the next section, we shall compute the compression between 5.2 GPa and 280 GPa, but especially focused on 243 GPa, the position of the melting point at the Hugoniot crossing.

We need a calculation of density vs P along the γ-phase solidus. We shall compute this empirically from the bulk modulus-pressure curve of the solidus, which is constrained by the K_S-P curves shown in Figure 7. The solid Hugoniot (in the ε-phase) is plotted below 200 GPa. The γ-phase solidus will have values of K_S larger than those shown for the outer core and smaller than those shown for ε-phase iron. The zero pressure values will be 136 GPa (Table 2), and K_S = 1150 GPa at P = 250 GPa. The behavior of the K_S-P curve between these values is not known, but it cannot depart much from a straight line because of the upper and lower constraints. Assume a straight line, so that

$$K_S = 136 + 4.05P \qquad (8)$$

Integrating this equation (since $K_S = \rho(\partial P/\partial \rho)_S$, we find that along the solidus

$$(\rho/\rho_o) = \left[1 + 4.05\frac{P}{(136)}\right]^{0.247} \qquad (9)$$

where ρ_o is the density at P = 0 and 1868°K. $V_{O\alpha}$ (α for the α-phase) is reported to be 7.09 cm^3/mole (ρ_o = 7.87 gm/cc) for iron at room temperature and pressure.

The zero pressure density in the liquid phase at high temperature (1868°K) is 7 gm/cm^3; or $V_{O\ell}$ = 7.97 cm^3/mole. Thus, $V_{O\ell}/V_{O\alpha}$ = 1.12. Now the initial density at the $\delta-\gamma-\ell$ triple point (at 5.2 GPa and 1970°K) is 7.25 gm/cm^3, or $V_{O\gamma-\delta-\ell}$ = 7.70 cm^3/mole. Thus, $V_{O\gamma-\delta-\ell}/V_{O\alpha}$ = 1.086.

We shall use $\gamma(5.2) = 1.95$ in (3) in the calculations of $T_m(P)$ along the $\gamma-\ell$ melting curve. A direct numerical integration, done by Anderson (1982), of (5) led to values of T_m at 250 GPa which fell within the error bars found by Brown and McQueen (1982) at 250 GPa, providing γ descended gradually from γ = 1.81 at 5.2 GPa to 1.0 at 320 GPa.

A more elegant way of integration was given by Spiliopoulos and Stacey (1984), in which (3) is replaced by

$$\frac{\partial \ln T_m}{\partial \ln \rho} = 2\left(\gamma - \tfrac{1}{3}\right) \qquad (10)$$

Now using the general relationship between γ and density

$$(\gamma/\gamma_o) = (\rho/\rho_o)^{-q} \qquad (11)$$

where q is an arbitrary constant (Anderson, 1968), and using (11) in (10), the integration yields

$$T_m/T_{m_o} = \left(\frac{\rho_o}{\rho}\right)^{2/3} \exp\left\{\frac{2\gamma_o}{q}\left[1-\left(\frac{\rho_o}{\rho}\right)^q\right]\right\} \qquad (12).$$

Equation (12) differs from Equation (2) of Spilioupolos and Stacey (1984) only in that their version has q = 1. The initial evaluation of (12) is not at P = 0, but at P = 5.2 GPa, the low pressure end of the γ-liquid phase boundary, so γ_o = 1.95 satisfies the conditions at the intitial point. Using (9) and (12), the temperature, pressure, and volume relationships are calculated along the γ-phase solidus. These calculations are shown in Table 3 and Figure 11.

Thermodynamic Properties of the γ-Liquid Phase Boundary

Between the Triple Points at 5.2 GPa and 280 GPa

P GPa	(ρ_1/ρ) $(\rho_1=7.25)$	V $(cm^3/mole)$	ρ gm/cm^3	T, °K (q = 1.5)	T (q = 1.8)	T q = (1.2)	γ (q = 1.5)
5.2	1.0	7.704	7.25	1970	1970	1970	1.95
25	0.902	6.945	8.04	2660	2650	2680	1.67
50	0.827	6.363	8.78	3317	3246	3360	1.46
75	0.775	5.966	9.36	3786	3679	3903	1.33
100	0.736	5.668	9.85	4183	4000	4360	1.20
125	0.706	5.441	10.76	4490	4263	4723	1.16
135	0.695	5.356	10.43	4596	4360	4863	1.13
150	0.680	5.235	10.67	4753	4487	5056	1.09
175	0.660	5.086	10.98	4965	4653	5325	1.05
200	0.641	4.937	11.31	5176	4803	5590	1.00
225	0.626	4.824	11.57	5338	4905	5805	0.97
243	0.615	4.732	11.80	5445	5014	5960	0.94
250	0.611	4.710	11.86	5497	5050	6009	0.93
280	0.595	4.590	12.18	5688	5140	6224	0.89

The three solutions shown bracket the experimental limits at 243 GPa found by Brown and McQueen. The only variable is q, the exponent in the power law. All other parameters satisfy the experimental data taken by static high pressure data at 5.2 to 10 GPa, and by shock wave data at 200-250 GPa. Thus, a reasonable Lindemann fit can be made for the γ-phase solidus curve.

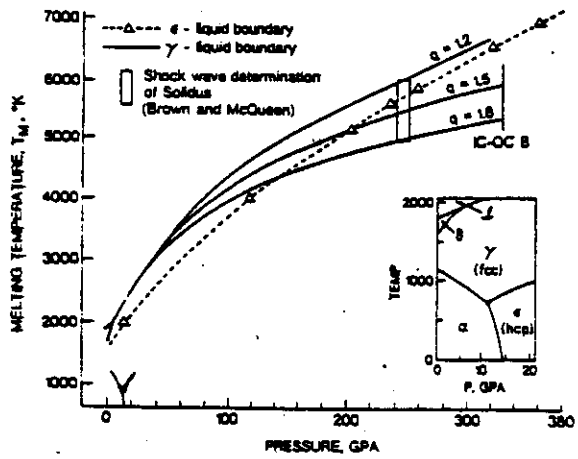

Figure 11. The melting curves of γ-iron which satisfy the static high pressure data (5.2 to 10 GPa) and the shock wave data (243 GPa), using a Lindemann law. The theoretical melting curve of ε-iron (Young and Grover, 1984) is shown for comparison. In the low pressure range, the γ-iron melting curve is required by the experiments.

F. The Grüneisen Parameter.

The solution for q = 1.5 yields temperatures which pass close to the midpoint of the pressure range reported by Brown and McQueen, (1982) at 200 GPa (5500 ± 500). Choosing this solution, and recalling that $\gamma_o = 1.95$ at the origin (P = 5.2 GPa), we have

$$\gamma = 1.95 \left(\frac{7.25}{\rho}\right)^{1.5} \qquad (13)$$

over the entire 280 GPa pressure range. At 280 GPa, we find $\gamma = 0.89$.

The value of q can be used as a control to meet any arbitrary value of T within the limits found by Brown and McQueen (1982) at 243 GPa. For q = 1.8, Eq. (12) gives a value close to 5000°, and for q = 1.2, Eq. (12) gives a value close to 6000°. Thus, the error bars can be placed on q: q = 1.5 ± 3.

A plot of the Grüneisen parameter vs V for the γ-phase-liquid boundary is given in Figure 12, according to values from Equation (13). They are compared with $\gamma\rho = 15$ used by Brown and McQueen (1982) and the later value, $\gamma\rho = 12$, also used by Brown and McQueen (1984). The values of γ determined numerically by Anderson (1982), to find the γ melting curve are close to the $\gamma\rho$ = constant solution (curve b).

The solution for q = 1.5 arises because the measured slope dT_m/dP of the γ-phase liquid boundary at 5.2 GPa is used to constrain the solidus as well as the shock wave measurements at 243 GPa.

There is no reason why the values of the Grüneisen parameter for the γ-phase should be identical to those of the α- or ε-phase. Nevertheless, the value of the Grüneisen parameter for the γ-phase at the volume of the standard pressure and temperature (7.094 cc/mole) yields $\gamma = 1.72$, which is very close to the room temperature, room pressure value of α-iron, measured by Ramakrishnan, et al., (1978) - (1.70). The values computed by (3) are somewhat lower than suggested by Jamieson, et al (1978) for iron at core conditions. (They found $\gamma = 1.2 - 2.$) Mulargia and Boschi (1977) derived values of γ (from a fundamental approach) which are in the same range as shown in Figure 12, although slightly lower. Spiliopoulos and Stacey (1984) used the solution $\gamma\rho = 15$ (curve a, Figure 12) to define the γ-phase solidus curve. The values of γ used by Anderson (1982) to find the solidus using Stevenson's version of the Lindemann law, (5), are close to the solution $\gamma\rho = 12$ (curve b, Figure 12).

Jeanloz (1979) found $\gamma = 2.2\ (\rho_{\alpha}/\rho)^{1.62}$ for the Hugoniot in the solid ε-phase field (ρ_{α} = 8.31 assumed), as shown in Figure 12. The theoretically calculated values of γ for the epsilon phase (Young and Grover, 1984), for the solidus, are shown in Figure 12. It is obvious that the values of γ for the epsilon phase are higher than the corresponding values for the gamma-phase liquid boundary. It is also apparent that the values of γ for the solidus are close to that of α-iron at room temperature.

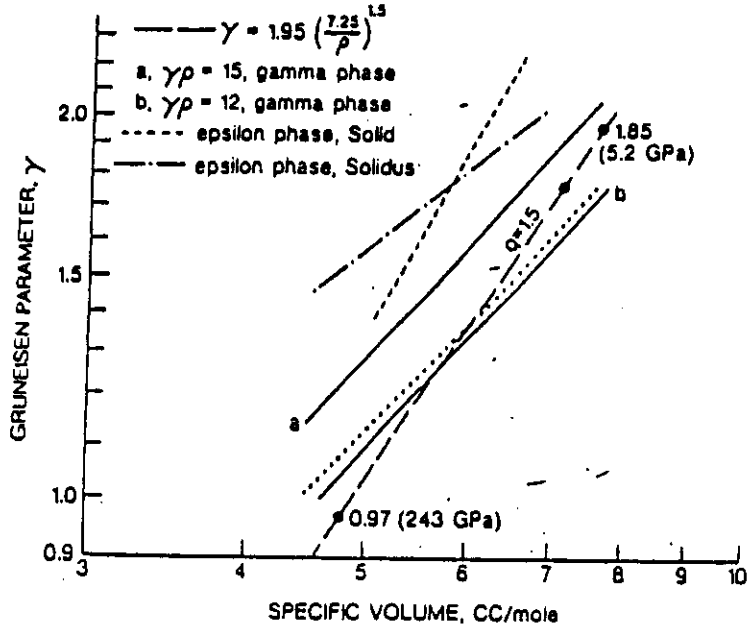

Figure 12. The Grüneisen parameter, γ, vs volume for the fcc phase of iron (γ). The dashed line is our solution for q = 1.5, the temperature curve in Figure 11 which bisects the measurements of the solidus at 243 GPa by Brown and McQueen (1983, 1984). The two solid lines represent solutions of the form $\rho\gamma$ = constant: curve a was used to calculate temperatures by Brown and McQueen (1984) and by Spiliopoulos and Stacey (1984), and curve b was used to calculate temperatures by Brown and McQueen (1984). The dotted line shows the values of γ, determined numerically by Anderson (1982), using Eq. (5).

The two upper curves are for epsilon-iron, one for the epsilon-phase in the solid, determined from the Hugoniot (Jeanloz, 1979), and the dot-dash is for the ε-phase liquid equilibrium boundary calculated theoretically (Young and Grover, 1984).

G. On the Question of the $\varepsilon-\gamma$ Phase Boundary.

a. The slope of the boundary of the $\varepsilon-\gamma$ solid-solid transition.

If a straight line is passed between the measurement of the maximum $\varepsilon-\gamma$ transition temperature allowed by the measurements at 200 GPa (4700°K) and the temperature at the $\alpha-\gamma-\varepsilon$ triple point, (750°K) at 11 GPa, the slope is 21°/GPa. The only measurement of this slope was by Bundy (1965), who found dT/dP = 28°/GPa at 11 GPa. The other properties of the t.p. convinced Liu (1975) that the slope was 31°/GPa. One estimate from Takahashi and Bassett (1964) represented the lowest estimate, 20°/GPa.

If we use the value dT/dP = 21°/GPa and extrapolate beyond the measured $\varepsilon-\gamma-\alpha$ transition at 11 GPa, then the temperature at 250 GPa is about 5700°. This solution would locate the triple point near the liquid boundary on the Hugoniot (250 GPa, 5500° K ± 500). If this were the case, the gamma phase is in equilibrium with the liquid at a pressure lower than that corresponding to a depth of 4100 km, and the epsilon-phase is in equilibrium with the liquid at higher pressures.

We have to consider the alternative, that dT/dP for the $\varepsilon-\gamma$ boundary is larger than 21°/GPa at 11 GPa, in respect of Bundy's (1965) measurement of this boundary (28°/GPa). In this case dT/dP must decrease with pressure in order to pass through the phase boundary measured by Brown and McQueen at 200 GPa (see Figure 9 for the transition).

In many solids, phase line slopes are reported to be constant with P, but in these cases, the compression is small compared to that of iron. A constant slope for the $\varepsilon-\gamma$ phase line over such a large compression may be possible, but alternates must be considered. Theoretical considerations indicate that for the NaCl-CsCl transition in alkali halides, ΔS is proportional to $(\Delta V)V_1$, where V_1 is the volume of phase 1 (Jeanloz, 1982). Moreover, it is even possible for $\Delta T/\Delta P$ to become negative before ΔV becomes vanishingly small (Bassett, et al., 1968).

The question for the iron $\varepsilon-\gamma$ transition is, does ΔS decrease as ΔV, or is it more like the case of the alkali halides, where ΔS decreases as $(\Delta V)V_1$, where V_1 is the volume of the lower phase in the transitions.

Assume that

$$\Delta S \approx (\Delta V)V^r$$

where r is independent of pressure. Then

$$dT/dP \propto V^r$$

or

$$\int dT = C\int_{P_1}^{P_2}\left(\frac{1}{\rho_o}\right)^{-P} dP \qquad (14)$$

Set C to $(dT/dP)_{(11)}$, the slope of the $\varepsilon-\gamma$ phase boundary evaluated at the triple point at 11 GPa.

Let us use the Murnaghan EOS relating density and pressure along an adiabat. This empirical relation satisfies both the lower mantle and outer core, because the bulk modulus is linear in P throughout the outer core and the lower mantle. (See Lecture 1.)

b. <u>The temperature-pressure relationship</u>.

Assume, then, the Murnaghan EOS, and Eq. (14) becomes

$$T_2 - T_1 = C\int_{P_1}^{P_2}\left[1 + K_o'\frac{P}{K_o}\right]^{-P/K_o} dP \qquad (15)$$

Consider K_o and K_o' for the ε-phase, from Table 2: The values K_o = 178 GPa and K_o' = 5.2 represent isothermal conditions. Now in changing from isothermal conditions, the value of K_o and K_o' must change, although the change is small.

Using the calculus formula

$$\left(\frac{\partial K_S}{\partial P}\right)_c = \left(\frac{\partial K_S}{\partial P}\right)_T + \left(\frac{\partial K_S}{\partial T}\right)_P \left(\frac{\partial T}{\partial P}\right)_c \qquad (16)$$

where the subscript c indicates core. We need to evaluate K_S at higher temperatures, and therefore need $(\partial K_S/\partial T)_P$ for ε-iron. For the α-phase $(\partial K_S/\partial T)_P$ is known, (- 0.018°/GPa), and for the ε-phase, it will be smaller.

Thus, $(\partial K_S/\partial T)_P$ is probably near - 0.015°/GPa. Along the phase boundary, $(\partial T/\partial P)_C$ varies between 20 and 30°/GPa. Take the average value $(\partial T/\partial P)_C$ = 25°/GPa. Thus, the last term in (16) is - 0.38. From the experimental data, $(\partial K_S/\partial P)_T$ is reported to be 5.2, but the error is significant, and as we shall see later, K_o may be higher than 5.2. Therefore, take $(\partial K_S/\partial P)_C$ = 5.0.

We need a value of K_o appropriate to some higher temperature. At the lowest limit of integration T = 750°K, so K_o must be appropriate to that of a T at least 750°K. Correcting from 300 to 750°, we find ΔK_S = 6 GPa. Thus, the values we use will be K_o = 170 and K_o' = 5.0. The empirical relationship of K to P for ε-iron along the γ-ε phase boundary becomes

$$K = 170 + 5P \qquad (17)$$

and this empirical law justifies the integrand in (15).

The solution to (15) is

$$T - T_o = C\frac{K_o}{K_o' - P}\left[\left\{1 + \frac{K_o'}{K_o}(P - P_o)\right\}^{1-\frac{r}{K_o'}} - 1\right] \qquad (18)$$

T_1 = 750°K.

Now C is reported to be 30°/GPa by Liu (1976), while only 20°GPa by Takahashi and Bassett (1964). Bundy's measurements indicate 28°/GPa. We shall use the midpoint between the highest and lowest, C = 25°/GPa as the first trial, where CK_o/K_o' = 25 x 170/5.0 = 25 X 170/5.0 = 850°.

We now solve (18) to find the value of r which yields T_2 = 4400 ± 300 at P_2 = 200 GPa, when T_1 = 750 at P_1 = 11 GPa. For r = 1, T_2 = 4408, which is the midpoint of the transition according to Brown and McQueen (1982). Thus, $\Delta S/\Delta V$ is proportional to V in this preferable case.

The equation

$$\Delta S \approx \Delta V^* V_1$$

satisfies the shock-wave data for the ε-γ phase boundary. The above is the same as found for the case of the B_1 - B_2 phase boundary in alkali halides (Jeanloz, 1982; Liu and Bassett, 1973).

The extreme lower case allowed by the data is found by using Bundy's measured value of the slope at 11 GPa (28^{o}/GPa), and requiring that it pass through the lower limit in T at 200 GPa (4100^{o}K). This yields r = 1.45. In that case, T(243) = 4108^{o}K; T(250) = 4813 and T(330) = 5832. This is shown in Figure 13.

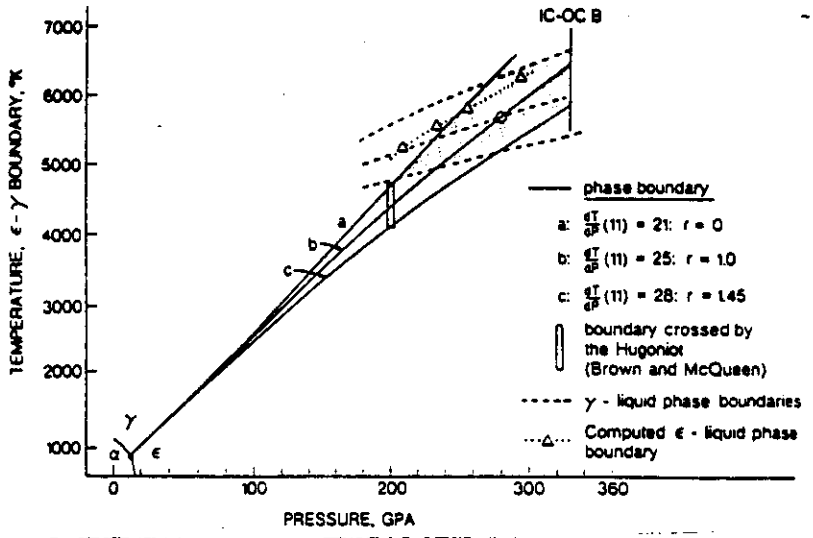

Figure 13. Calculated phase boundaries of the ε-γ iron equilibrium curves for three slopes extending from the (α-ε-γ) triple point: Case a is for 21^{o} GPa, which is a straight line intersecting the upper limit of the experimental determination by Brown and McQueen. Case b is for 25^{o} GPa, the median allowed slope; it passes through the midpoint of the experimentally determined window if r = 1.0 (Equation (21). Case c is for 28^{o}GPa, the slope measured by Bundy; it passes through the lowest point of the experimentally determined window if r = 1.45 (Eq. (14)). The (ε-γ-liquid) triple point lies in the cross-hatched area.

C. The EOS for the ε-γ phase boundary.

Assume the P-T relationship is given by (18). We now calculate the density consistent with these values. Assume the general EOS.

$$P = P_{ISO} + P_{TH} .$$

where P_{ISO} is along the 0^{o}K isotherm, and P_{TH} is along an isochore. For P_{TH}, use (39) of Lecture 1, and

for P_{ISO}, use the Birch-Murnaghan EOS (Eq. (50) of Lecture 1). Thus

$$P = \frac{3}{2} K_0 \left\{ \left(\left(\frac{\rho}{\rho_0}\right)^{7/3} - \left(\rho/\rho_0\right)^{5/3} \right) \left\{ 1 + \frac{3}{4}\left(K_0' - 4\right)\left[\left(\rho/\rho_0\right)^{2/3} - 1 \right] \right\} \right\}$$

$$+ \frac{\gamma \rho}{55.83} 3RT \qquad (19)$$

For the γ_{ac} relationship, use that for iron in the solid ε phase found by Jeanloz (1979) (see Figure 12).

$$\gamma = 2.2 \left(\frac{8.31}{\rho} \right)^{1.62} \qquad (20)$$

The thermal pressure becomes

$$P_{TH} = 0.03036 \rho^{-0.62} T \text{ GPa}$$

Using the zero degree parameters for (19) given by

$$\rho_0 = 8.29 \text{ gm/cm}^3 ; \quad K_0 = 180 \text{ GPa} , \quad K_0' = 5.2,$$

the thermal EOS becomes

$$P = 0.4266 \rho^3 - 1.553 \rho^{2.333} - 0.7952 \rho^{1.667} + 0.0304 \rho^{-0.62} T \qquad (21).$$

For a given P, a value of T is found from (18). For the set of values of P and T, a value of ρ is found, satisfying (21). The results of the calculations are given in Table 4.

We have used the Birch-Murnaghan EOS for the P-ρ relationship in (19), but the Murnaghan EOS for the P-ρ relationship in (18). At first this appears inconsistent. However, the Murnaghan EOS is not used along an isotherm, because T depends upon P in (18). The Birch-Murnaghan EOS, as used in (19) is along the 0°K isotherm.

Table 4

Thermodynamic Properties of Fe at the γ-ε Phase Boundary Between the Triple Points at 11 GPa and 280 GPa

P (GPa)	T (°K)	ρ (gm/cm³)	V (cm³/mole)	V/V₀ (V₀=7.094 cm³/mole)	γ
11	750	8.505	6.564	0.9253	2.119
25	1087	8.74	6.265	0.8803	1.954
50	1639	9.57	5.834	0.8224	1.750
75	2152	10.10	5.528	0.7792	1.604
100	2637	10.55	5.292	0.7460	1.495
125	3101	10.95	5.099	0.7187	1.407
135	3281	11.10	5.030	0.7090	1.378
150	3548	11.31	4.936	0.6958	1.335
175	3981	11.645	4.794	0.6758	1.274
200	4403	11.95	4.672	0.6586	1.221
225	4814	12.235	4.563	0.6432	1.176
243	5105	12.43	4.492	0.6331	1.146
250	5217	12.505	4.465	0.6294	1.135
280	5690	12.805	4.360	0.6146	1.092

H. The (ε, γ, ℓ) triple point.

a. Temperature at the IC-OC Boundary.

The triple point (t.p.) occurs somewhere in the cross hatched area shown in Figure 13. There are two likely choices for the coordinates. The first, determined from the experimental evidence, is the crossing of the bisectors of the experimental error rectangles: curve b in Figure 13 with the q = 1.5 solution in Figure 11. The second, leaning toward the theoretical solution of the ε-phase-liquid boundary (Young and Grover, 1984), would be somewhere on the dotted line of Figure 13, between 260 GPa and 310 GPa. We choose the former, locating the triple point at 280 GPa and 5690°K.

Data on the γ-liquid branch and the ε-γ branches of the t.p. are determinable from measurements and assumptions made to this point. For the ε-liquid branch, some additional assumptions must be made.

At the IC-OC boundary pressure, the upper temperature limit is 6600°K, as given by Young and Grover (1984), and the lower limit is 5960°K, as given by the intersection of the q = 1.5 curve of Figure 11 with the IC-OC boundary pressure. The midpoint is 6280°C. Close to the extrapolated point of curve b of Figure 13, we choose T(330) = 6280 ± 400, giving a slope of dTm/dP = 11.8°/GPa for the ε-liquid phase boundary. This lies between the value found from Young and Grover's theory (13.8°/GPa) and the value found from the solution γρ = 15 (8.°/GPa).

This solution, (6280 ± 400), is close to that found by Spiliopoulos and Stacey (1984) (6120 ± 575). The approaches are quite different, however. For example, in the Spiliopoulos and Stacey solution, the inner core is in the γ-phase of iron (e.g., there is no high triple point at core pressure) whereas in this solution the inner core is in the ε-phase.

Other predictions of the temperature at the IC-OC boundary are shown in Table 5.

The higher slope for the ε-phase liquid boundary, as compared to the γ-phase liquid boundary, is a reflection of the higher values of γ found for the epsilon phase as compared to the γ-phase (see Figure 12).

Table 5. Predicted Temperatures of the Melting Point of Pure Iron at the Pressure of the Inner-Outer Core Boundary

	T_m/K
Gilvary, 1957	6200
Zharkov, 1962	6200
Bundy & Strong (1962)†	6100-8100
Higgens & Kennedy (1971)†	4250
Birch (1972)†	5100
Leppaluoto	7000-9000
Boschi*	6600
Liu (1975)**	5125
Boschi, et al. (1979)*	4500-7000
Abelson (1981)**	7800
Stevenson (1981)	6300
Brown & McQueen (1982)***	6200 ± 500
Anderson (1982)***	5900 ± 700
Brown & McQueen (1984)***	5800 ± 500
Spiliopoulos & Stacey (1984)***	6140 ± 575
Young & Grover (1984)	6600
This report***	6280 ± 400

† Based upon an extrapolation from experiments at 6 GPa.
* A special case of the Ross theory (1969).
** Based upon Monte Carlo theory.
*** Based upon an extrapolation from experiments at 243 GPa.

It is somewhat remarkable how many scientists have successfully predicted that T_m is near 6200° at the IC-OC Boundary, in advance of the measurements of Brown and McQueen (1982).

b. <u>The γ-ε Branch</u>.

At the triple point, the following must be satisfied: $\Sigma \Delta V = 0$ and $\Sigma \Delta S = 0$, in a circuit around the triple point.

To find the slope dT/dP at the triple point, we need values of T, K, and γ. From data on the Hugoniot, Figure 6, we find $K_S(280) = 1270^o$ GPa.

From (10) we find $\gamma(280) = 0.89$, taking $\rho(280) = 12.16$, $K_S = 1270$. Calculating $T_m(280) = 5688^oK$ from (19) (for the case $q = 1.5$), we find from (3)

$$\left(\frac{dT_m}{dP}\right)_{\gamma-1}(280) = 5^o/GPa \qquad (22)$$

Using the Clasius-Clapyron relationship,

$$\Delta T_m/\Delta P = \Delta S_m/\Delta V_m \qquad (23)$$

ΔV_m can be determined from a calculation of ΔS_m.

Following the procedure presented by Spiliopoulos and Stacey (1984), we include the important term, the configurational entropy, ΔS_c, so that

$$\Delta S_m = \Delta S_c + \left(\frac{\partial S}{\partial V}\right)_T \Delta V_m \qquad (24)$$

The following is a thermodynamic identity

$$\left(\frac{\partial S}{\partial V}\right)_T \equiv \left(\frac{\partial P}{\partial T}\right)_V = \alpha K_T \qquad (25)$$

where K_T is the isothermal bulk modulus. By using the Grüneisen parameter relationship

$$\gamma = \frac{\alpha K_T}{\rho C_V} \qquad (26)$$

in (25),

$$\left(\frac{\partial S}{\partial V}\right)_T = \rho \gamma C_V$$

Combining (27), (24) and (23), as shown by Spiliopoulos and Stacey (1982),

$$\left[\left(\frac{\partial P}{\partial T}\right)_m - (\rho\gamma)_m C_{V_m}\right]^{-1} = \frac{\Delta V_m}{\Delta S_c} \qquad (27)$$

Now C_{V_m} at the triple point can be computed from (5), since all variables are known from the computation leading to (27). Using (27) and $\gamma = 0.85$ with $K_m = 1200$, we find $C_V^{vib} = 2.98R$, which is close enough to the classical limit.

The value of $\gamma\rho = 0.89 \times 12.16 = 10.84$ gm/cm^3. Thus

$$(\rho\gamma)_m C_{V_m} = 10.84 \times 5.98 \times \frac{1}{55.83}$$

$$= 1.18 \ \frac{Cal}{deg\ cm^3}$$

Converting (22) to the same units

$$\left(\frac{dP}{dT}\right)_m = \frac{1}{5} \times \frac{10^3}{4.193}$$

$$= 48.1 \ Cal/cm^3 deg$$

Thus

$$\left(\frac{dP}{dT}\right)_m - (\rho\gamma)_m C_{V_m} = 46.8 \ \frac{Cal}{cm^3 deg} \qquad (28)$$

and

$$\Delta V_{m(\gamma-\ell)}(280) = \frac{\Delta S_{c(\gamma-\ell)}}{46.8} \ \frac{cm^3}{mole} \qquad (29)$$

It is well known that the configurational entropy changes little with pressure (Slater, 1939), so ΔS_c can be estimated at low pressure methods using statistical methods (Slater, 1939). We adopt the estimate of Spiliopoulos and Stacey (1984), $\Delta S_c = 129$ J Kg^{-1} deg^{-1} = 1.72 cal/mole degree = 0.86 entropy units. This number is to be compared to the extrapolated value of entropy at high pressure made by Stishov (1975), using his measurements on alkali metals, $\Delta S_c/R = \ln 2 = 0.693$ e.u.

From this result, we find from (32)

$$\Delta V_{m(\gamma-\ell)}(280) = \frac{1.72}{46.8} = 0.037 \ \frac{cm^3}{mole}$$

and $\Delta S_m(280) = 1.72 + 1.18 \times 0.037 = 1.77$ cal/mole degree.

The relative change of volume at 280 GPa is 0.037/4.59 = 1%, which agrees with the estimate of Brown and McQueen (1982) at 250 GPa.

c. The $\varepsilon \rightarrow \gamma$ Branch and the $\varepsilon \rightarrow \ell$ Branch at the Triple Point.

We now proceed to estimate ΔV and ΔS for the $\varepsilon \rightarrow \gamma$ branch of the transition.

To calculate dT_m/dP, we use solution b of Figure 12 and find

$$\left(\frac{dT_m}{dP}\right)_{\epsilon-\gamma} = 15.3 \pm 4\ ^\circ/\text{GPa} \qquad (30)$$

Mao, et al., (1967) reported that $\Delta V(\gamma \rightarrow \varepsilon)$ at 11 GPa is 0.13cm^3/mole. Taking (dT/dP)(11) = 25°/GPa, we find

$$\Delta S_{\varepsilon-\gamma}(11) = \frac{0.13 \times 1000}{25 \times 4.186} = 1.24 \ \frac{\text{cal}}{\text{mol deg}}$$

= 0.62 entropy units.

There are four unknowns remaining at the 280 GPa t.p.: $\Delta S_{\varepsilon \rightarrow \gamma}$; $\Delta S_{\ell \rightarrow \varepsilon}$; $\Delta V_{\varepsilon \rightarrow \gamma}$; and $\Delta V_{\ell\varepsilon}$.
There are also four equations to find these unknowns.

$$\frac{\Delta V_{\epsilon-\gamma}}{\Delta S_{\epsilon-\gamma}} = \left(\frac{dT_m}{dP}\right)_{\epsilon-\gamma} = 15.3\ ^\circ/\text{GPa} \qquad (31)$$

$$\frac{\Delta V_{\ell-\epsilon}}{\Delta S_{\ell-\epsilon}} = \left(\frac{dT_m}{dP}\right)_{\ell\epsilon} = 11.8\ ^\circ/\text{GPa} \qquad (32)$$

$$\Delta V_{\epsilon-\gamma} + \Delta V_{\ell-\epsilon} = -(\Delta V_{\gamma-\ell}) = -0.037\ \text{cm}^3/\text{mole} \qquad (33)$$

$$\Delta S_{\epsilon-\gamma} + \Delta S_{\ell-\epsilon} = -(\Delta S_{\gamma-\ell}) = -1.77\ \text{cal/mole deg} \qquad (34)$$

Solving these equations we find

$$\Delta S_{\varepsilon \rightarrow \gamma} = 3.44 \text{ cal/mole deg.} = 14.39 \text{ J. mole}^{-1} \text{ deg}^{-1} \qquad (35)$$

$$\Delta S_{\varepsilon \rightarrow \ell} = 5.21 \text{ cal/mole deg.} = 21.76 \text{ J. Mole}^{1} \text{ deg.}^{-1} \qquad (36)$$

$$\Delta V_{\varepsilon \rightarrow \gamma} = 0.221 \text{ cm}^3\text{/mole} \qquad (37)$$

$$\Delta V_{\varepsilon \rightarrow \ell} = 0.258 \text{ cm}^3\text{/mole} \qquad (38)$$

This shows that ΔS drops somewhat along the γ-ϵ phase boundary. The ΔV changes from 0.40 cm^3/mole at 11 GPa to 0.221 cm^3/mole at 280 GPa along the ϵ-γ boundary.

The thermodynamic data for these three triple points are given in Table 6. Data for the lower triple points are calculated by the same method as used above for the high triple point.

Table 6
Solutions for the Volume and Entropy Changes at Triple Points

	P (GPa)	T (°K)	ΔV (cm^3/mole)		ΔS (cal/mole deg) (e.u.)	dT/dP (°K/GPa)
(α-γ-ϵ)t.p.						
Alpha-gamma	11	750	-0.90	+8.60	+4.43	-25
Gamma-epsilon	11	750	-0.30	-2.87	-1.48	+25
Epsilon-alpha	11	750	+1.20	-5.73	-2.95	-50
(γ-δ-liq.)t.p.						
Liquid-gamma	5.2	1970	-0.5		-1.50	+40
Gamma-delta	5.2	1970	+0.08		+0.14	+70
Delta-liquid	5.2	1970	+0.42		+1.38	+37
(ϵ-γ-liq.)t.p.						
Epsilon-gamma	280	5690	+0.221	+3.44	+1.77	+15.3
Gamma-liquid	280	5690	+0.037	+1.77	+0.91	+5.0
Liquid-epsilon	280	5690	-0.258	-5.21	-2.68	+11.8
Birch (1972)						
Alpha-gamma	0	1184	-0.075			-40
Gamma-delta	0	1665	0.042			+52
Delta-liquid	0	1808	0.28			+26

I. The Phase Diagram of Iron.

Using the data of the previous sections, the phase diagram of iron is constructed. For this purpose we shall use the γ-phase liquid boundary corresponding to $\gamma = 1.5$ (Figure 11) and the γ-phase ϵ-phase boundary corresponding to b of Figure 13 ($\Delta S \curvearrowleft \Delta V \bullet V$), in which the triple point is at 280 GPa and 5690° K. We also select $dT_m/dP = 11.8°$/GPa for the ϵ-phase liquid boundary yielding 6280° at 330 GPa.

The resulting T-P diagram is given in Figure 14.

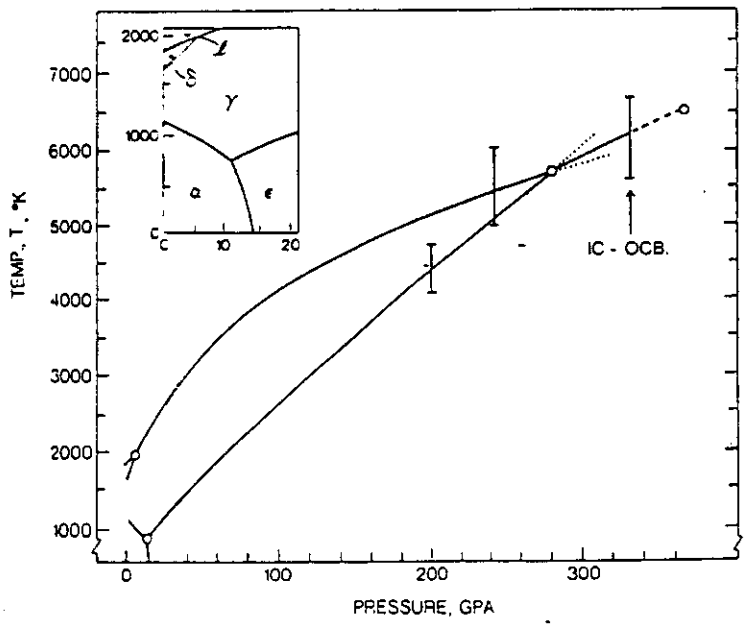

Figure 14. The temperature-pressure phase diagram of iron (see text for description).

The resulting V-T diagram is given in Figure 15. It is seen that the melting curve is concave upward, in contrast to the straight line previously assumed by several authors, who followed the Kraut-Kennedy relationship (1966), where it was assumed that $T_m \sim \Delta V/V_o$. For example, Birch's (1972) projection of the low pressure data by a straight line yields a lower temperature (5100°K) at 330 GPa, than found by using the shock wave data (see Table 5 and Figure 14).

The adiabat for the liquid is shown by the dashed line, fixed to a solid-liquid boundary at 330 GPa. The fundamental equation is given by

$$dT_m/dP = K/T_m\gamma$$

and the temperature is determined by integration using the same values of the gammas as used in the construction of the solidus on both sides of the triple point.

Using the data in Table 5, and taking $\gamma = 1.45$ for the ε-phase liquid boundary (280-330 GPa), we find the density at the inner-outer core boundary to be 12.9

gm/cc. The ΔV at this boundary is 0.08 cm^3/mole at the triple point, so 12.82 would represent the density at the solid side. This agrees well with the density of the inner-core side of the inner-outer core boundary measured by seismology, which is 12.76 according to the PREM model (Dziewonski and Anderson, 1981) and 13.34, according to the Cal 8 model (Bolt, 1982).

The change of density across the inner core is 2.6%, so we might expect $\Delta T/T$ across the inner core to be 4%, using $\gamma = 1.5$ (Jamieson, et al., 1978) or 4.7%, using $\gamma = 1.8$ (Bukowinski, 1977). Thus, the temperature at the center of the Earth is about 6550°K, with wide limits of error.

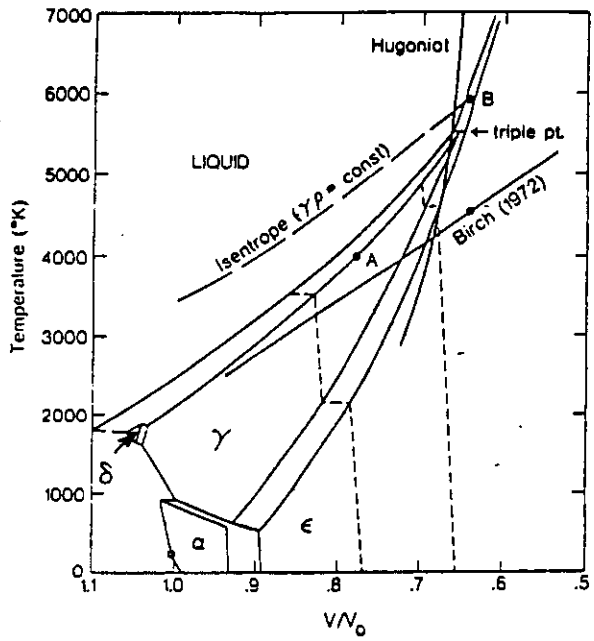

Figure 15. The temperature-pressure phase diagram of iron (see text for description).

References

Abelson, R.S., Ph.D. thesis, University of California at Los Angeles, 1981.

Ahrens, Thomas J., Equations of state of iron sulfides and constraints on the sulfur content of the Earth, J. Geophys. Res., 84, 985-998, 1979.

Ahrens, Thomas J., Dynamic compression of Earth materials, Science, 207, 1035-1040, 1980.

Al'tshuler, L.V., S.B. Kormer, M.I. Braznik, L.A. Vladimirov, M.P. Speranskoya and A. I. Funtkov, The isentropic compressibility of aluminum, copper, lead and iron at high pressures, Sov. Phys. JETP, 11, 766-775, 1960.

Al'tshuler, L.V. and S.B. Kormer, On the internal structure of the Earth, Isv. Acad. Sci., USSR Geophys. Ser., 1, 18-21, 1961.

Al'tshuler, L.V., A. A. Bakanova and R.F. Trunin, Shock adiabats and zero isotherms of seven metals at high pressures, Sov. Phys., JETP, 15, 65-74, 1962.

Al'tshuler, L.V., G. V. Sinakov and R.F. Trunin, On the composition of the Earth's core, Izv. Earth Phys., 1, 1-3, 1968.

Al'tshuler, L.V., M.I. Brazhnik and G.S. Telgrin, Strength and elasticity of iron and copper at high shock-wave compression pressures, J. App. Mech. Tech. Phys., 12, 921-926, 1971.

Anderson, D.L. and O.L. Anderson, The bulk modulus-volume relationship for oxides, J. Geophys. Res., 75, 3493, 1970.

Anderson, O.L., A proposed law of corresponding states for oxide compounds, J. Geophys. Res., 71, 4963-4971, 1966.

Anderson, O.L., Some remarks on the volume dependence of the Grüneisen parameter, J. Geophys. Res., 73, 51, 1968.

Anderson, O.L., The Earth's core and the phase diagram of iron, Phil. Trans. R. Soc. London, A, 306, 21-35, 1982.

Andrews, D.J., Equation of state of the alpha and epsilon phases of iron, J. Phys. Chem. Solids, 34, 825-840, 1973.

Bassett, W.A., T. Takahashi, H. Mao, and J.S. Weaver, Pressure-induced phase transformation in NaCl, J. Appl. Phys., 39, 319-325, 1968.

Birch, F., Elasticity and constitution of the Earth's interior, J. Geophys. Res., 57, 227-286, 1952.

Birch, F., Some geophysical applications of high-pressure research, in Solids Under Pressure, edited by W. Paul and D.M. Warschauer, McGraw-Hill, New York, 1963.

Birch, F., The melting relations of iron, and temperatures in the Earth's core, Geophys. J. R. Astr. Soc., 29, 373-387, 1972.

Bolt, B.A. and R. A. Uhrhammer, The structure, density and homogeneity of the Earth's core, Evolution of the Earth, edited by R. J. O'Connell and W.S. Fyfe, Geodynamics Series, Volume 5, pp. 28-38, Washington, D.C.: American Geophysical Union, 1981.

Bolt, B.A., Inside the Earth, Table 4, San Francisco: W. H. Freeman and Co., 1982.

Boschi, E., The melting relations of iron and temperatures in the Earth's core, Riv. Nuovo Cim., 5, 501-531, 1975.

Boschi, E.F. Mulargia and M. Bonafede, The dependence of the melting temperature on the choice of the interatomic potential, Geophys. J. Roy. Astron. Soc., 58, 201-208, 1979.

Brett, R., The current status of speculations on the composition of the core of the Earth, Rev. Geophys. Space Phys., 14, 375-383, 1976.

Brown, E. and R.G. McQueen, Melting of iron under core conditions, Geophys. Res. Lett. 7, 533-536, 1980.

Brown, E. and R.G. McQueen, The equation of state for iron and the Earth's core, in High Pressure Research in Geophysics, edited by A. Akimoto and M. Manghnani, Tokyo: Center for Academic Publications, pp. 611-625, 1982.

Brown, E. and R.G. McQueen, Phase transition, Grüneisen parameter and elasticity for shocked iron between 100 GPa and 400 GPa, J. Geophys. Res., in press, 1984.

Bukowinski, M., A theoretical equation of state for the inner core, Phys. Earth Planet Inter., 14, 333-347, 1977.

Bundy, F.P. and H.M.Strong, Behavior of metals at high temperature and pressure, in Solid State Physics, edited by F. Seitz and D. Turnbull, vol. 13, pp. 81-143, New York: Academic Press, 1962.

Bundy, F.P., Pressure-temperature phase diagram of iron to 200 kbar, 900° C, J. Appl. Phys. 36, 616-620, 1965.

Davies, G.F., Elasticity, crystal structure and phase transitions, Earth Planet. Science Letters, 22, 239-241, 1974.

Dziewonski, A.M. and D.L. Anderson, Preliminary reference Earth model, Phys. Earth Planet. Inter., 25, 297-356, 1981.

Filipov, S.I., N.B. Kazakov, and L.A. Pronin, Velocities of ultrasonic waves, compressibility of liquid metals, and their relation to various physical properties (in Russian), Izv. Vyssh. Uchebn., Zaved. Chern. Metall., 9, 8-14, 1966.

Ganapathy, R. and E. Anders, Bulk compositions of the Moon, Earth, estimated from meteorites, Geochemica et Cosmochemica, Supp, 5, 1181-1206, 1976.

Gilbert, J.F. and A.M. Dziewonski, An application of normal mode theory to the revival of structural parameters and source mechanisms from seismic spectra, Phil Trans Roy. Soc. London, A., 178, 187-269, 1975.

Gilverry, J.J., Temperatures of the Earth's interior, J. Atmos. and Terr. Phys., 10, 84-95, 1957.

Grover, R., Liquid metal equation of state based on scaling, J. Chem. Phys., 55, 3435-3441, 1971.

Guinan M.W. and D.N. Beshers, Pressure derivatives of the elastic constants of α-iron to 10 kbs., J. Phys. Chem. Solids, 29, 541-549, 1968.

Hart, R.S., D.L. Anderson, and H. Kanamori, The effect of attenuation in gross Earth models, J. Geophys. Res., 82, 1647-1654, 1977.

Higgens, G. and Kennedy, G.C., The adiabatic gradient and the melting point gradient in the Earth's core, J. Geophys. Res., 76, 1870-1878, 1971.

Jamieson, J.C., H.H. Demarest, and D. Schiferl, A re-evaluation of the Grüneisen parameter for the Earth's core, J. Geophys. Res., 83, 5929-5935, 1978.

Jeanloz, R., Properties of iron at high pressure and the state of the core, J. Geophys. Res., 84, 6059-6069, 1979.

Jeanloz, R., Effect of coordination change on thermodynamic properties, in High Pressure Research in Geophysics, edited by A. Akimoto and M. Manghnani, pp. 479-498 Tokyo: Center for Academic Publishing, 1982.

Kraut, E.A. and G.C. Kennedy, New melting law at high pressure, Phys. Rev., 451, 668-675, 1966.

Kurz, W. and B. Lux, Die schallengeschwindigkeit von eisen und eisenlegierungen im festen und flussigen zustand, High Temp. High Pressures, 1, 387-399, 1969.

Leppaluoto, D.A., Melting of iron by significant structure theory, Phys. Earth Planet. Inter., 6, 175-181, 1972.

Lindemann, F.A., Über die Berechnung molecularer eigenfrequenzen, Phys. Zeits., 11, 609-612, 1910.

Liu, L. and W. A. Bassett, Compression of Ag and phase transformation of NaCl, J. App. Phys., 44, 1475-1479, 1973.

Liu, L., On the (γ, ε, ℓ) triple point of iron and the Earth's core, Geophys. J. R. Astr. Soc., 43, 697-705, 1975.

Lyttleton, R.A., On the origin of mountains, Proc. Roy. Soc. London A, 275, 1-22, 1963.

Lyttleton, R.A., On the phase change hypothesis of the structure of the Earth, Proc. Roy. Soc. A., 287, 471-493, 1965.

Mao, H.K. and Bell, P.M., Equations of state of MgO and ε Fe under static pressure conditions, J. Geophys. Res., 84, 4533-4536, 1979.

McQueen, R.G. and S.G. Marsh, Equation of state for nineteen metallic elements from shock wave experiments to two megabars, J. App. Phys., 31, 1253-1263, 1960.

McQueen, R.G. and S.P. Marsh, Shock-wave compression of iron-nickel alloys and the Earth's core, J. Geophys. Res., 71, 1751-1759, 1966.

McQueen, R.G., S.D. Marsh and J.N. Fritz, Hugoniot equations of state for 12 rocks, J. Geophys. Res., 72, 4999-5036, 1967.

McQueen, R.G., S.P. Marsh, J.W. Taylor, J.N. Fritz, and W.J. Carter, The equation of state of solids from shock wave studies, in High Velocity Impact Phenomena, edited by R. Kinslow, pp. 293-413 and appendices, New York: Academic Press, 1970.

McQueen, R.G. and S.P. Marsh, Shock wave compression of iron nickel alloys and the Earth's core, J. Geophys. Res., 84, 6059-6069, 1979.

Mulargia, F. and E. Boschi, Grüneisen's gamma function for liquid iron at the Earth's outer core conditions, Ann. Geophys., 30, 205-222, 1977.

Pavlovskii, A.I., N.P. Kolokolchiv, M.I. Dolotenko and A.I. Bykov, Isentropric compression of quartz by the pressure of a superstrong magnetic field, JETP Letters, 27, (English translation), 264-266, 1978.

Ramakrishnan, J., R. Boehler and G.C. Kennedy, Behavior of Grüneisen parameter of some metals at high pressure, J. Geophys. Res., 83, 3535-3538, 1978.

Ramsey, W.R., On the nature of the Earth's core, Monthly Notice Roy. Astron. Soc., Geophys. Supp., 5, 409-426, 1949.

Ramsey, W.R., On the compressibility of the Earth, Monthly Notice Roy. Astron. Soc., Geophys. Supp., 6, 42, 1950.

Ross, M., Generalized Lindemann law, Phys. Rev., 184, 233-241, 1969.

Ross, T.E. and L.H. Aller, The chemical composition of the Sun, Science, 191, 1223-1229, 1976.

Rotter, C.A. and C.S. Smith, Ultrasonic equation of state of iron, 1, low pressure, room temperature, J. Phys. Chem. Solids, 27, 267-276, 1966.

Shankland, T.J., Velocity density systematics, J. Geophys. Res., 77, 3750-3760, 1972.

Slater, J.C., Introduction to Chemical Physics, First edition, New York: McGraw Hill Book Co., Inc., 1939.

Spiliopoulos, S. and F.D. Stacey, The Earth's thermal profile: Is there a mid-mantle thermal boundary layer?, J. of Geodynamics, 1, 61-77, 1984.

Stacey, F.D. and R.D. Irvine, Theory of melting: Thermodynamic basis of Lindemann's law, Australian J. Physics, 30, 631-640, 1977.

Stacey, F.D., A thermal model of the Earth, Phys. Earth Planet. Inter., 15, 341-348, 1977.

Stevenson, D., Applications of liquid state physics to the Earth's core, Phys. Earth Planet. Inter., 22, 42-52, 1980.

Stevenson, D.J., Models of the Earth's core, Science, 214, 611-618, 1981.

Stishov, S.M., The thermodynamics of melting of simple substances, Sov. Phys. USP, 17, 625-643, 1975.

Strong, H.M., The experimental fusion curve of iron to 96,000 atmospheres, J. Geophys. Res., 64, 653-660, 1959.

Strong, H.M., R.E. Tuft, and R.E. Hannemann, The iron fusion curve and the γ-δ-ℓ triple point, Metall. Trans., 4, 2657-2661, 1963.

Takahashi, T. and Bassett, W.A., High-pressure polymorph of iron, Science, 145, 483-486, 1964.

Trunin, R.F., G.V. Simaleov, M.A. Podurets, B.N. Moiseev and L.V. Popov, Dynamic compressibility of quartz and quartzite at high pressures, Bulletin Acad. of Sciences USSR, Physics of the Solid Earth, 1, Jan. 1971, 8-12, (English translation).

Verhoogen, J., Energetics of the Earth, Washington, D.C.: National Academy of Science, 1980.

Wasson, John T., Meteorites, Appendix D, New York: W. H. Freeman, 1984.

Young, D.A. and R. Grover, Theory of the iron equation of state and melting to very high pressures, Proc. APS 1983 Topical Conference on Shock Waves in Condensed Matter, edited by J. Asay, American Physical Society, in press, 1984.

Zharkov, V.N., Physics of the Earth's core, (trans.) (Trudy), Institute of Earth Phys., Acad. Sci., USSR, 20, 187, 1962.

The Equation of State of the Earth's Outer Core

A. The Pressure of ε-iron at Inner Core Pressure.

The question we wish to examine is: Does the pressure of the ε-phase computed at inner core temperature and density conditions correlate well with the pressure there as determined from seismology studies?

A chief difficulty here is that there is not general agreement about the density of the inner core among seismologists. For example, the QM_2 model of Jordan and Anderson (1974) has virtually no jump in density at the inner-outer core boundary, while the PREM model shows a jump of 0.63 gm/cm^2, and as the extreme case, the CAL 8 model (Bolt, 1980) shows a jump of 1.17 gm/cm^2. Here we will use the CAL 8 model and the PREM model as upper and lower limits.

The choice of the best seismic model for the inner core will not be made here; that decision is a seismological question. But we note that it is extremely difficult to choose between models of the core based upon the geodetic and cosmological boundary conditions. The mass and moment of inertia of the inner core make only a very small contribution to M and I of the whole Earth. The difference between the jump in ρ from one model to another quoted above is not easily determined from the Earth's boundary conditions.

Table 1 shows the velocities, densities and pressure of CAL 8 and PREM for the inner core.

Table 1. Comparison of Density and Seismic Velocities Between the CAL 8 Model and PREM for the Earth's Core (Bolt, 1982)

Depth	Density		Comp. Velocity, Vp Km/sec		Shear Velocity Km/sec		Pressure GPa	
Km	CAL 8	PREM	CAL 8	PREM	CAL 8	PREM	CAL 8	PREM
2885	5.92	5.57	13.37	13.72	6.96	7.26	135.3	135.8
2885	9.82	9.90	8.09	8.06	0	0	135.3	135.8
3000	10.01	10.07	8.27	8.25	0	0	147.4	147.2
3200	10.33	10.37	8.56	8.56	0	0	168.3	168.1
3400	10.62	10.54	8.84	8.83	0	0	188.7	188.6
3800	11.11	11.11	9.33	9.31	0	0	227.9	227.5
4200	11.52	11.51	9.74	9.69	0	0	263.8	263.1
4550	11.84	11.79	10.00	9.97	0	0	291.8	290.7
4800	12.03	11.97	10.12	10.14	0	0	309.7	318.0
5000	12.14	12.09	10.18	10.27	0	0	322.5	320.4
5155	12.17	12.17	10.19	10.36	0	0	331.5	328.9
5155	13.34	12.76	10.89	11.03	3.49	3.50	331.5	328.9
5200	13.38	12.79	10.94	11.05	3.50	3.52	334.2	331.6
5400	13.49	12.88	11.13	11.11	3.55	3.56	345.1	341.5
5600	13.55	12.96	11.24	11.17	3.58	3.60	354.1	349.7
6200	13.59	13.08	11.33	11.26	3.60	3.66	368.9	363.1
6371	13.58	13.09	11.33	11.26	3.60	3.67	369.9	363.9

There is a small difference between the pressure of the PREM model and the Cal 8 model, but the difference in the density is larger.

To proceed, we need to estimate the thermal pressure at outer core conditions. With this calculation, we need an estimated value of the Grüneisen parameter and the outer core temperature.

From the velocity and density data, we may estimate the lattice Grüneisen parameter, using the formula presented in Lecture 1.

$$\gamma_{ac} = \frac{1}{3}\left(2\gamma_s + \gamma_p\right) \qquad (1)$$

where

$$\gamma_{s,\rho} = \frac{1}{3} + \frac{d \ln v_{s,\rho}}{d \ln \rho} \qquad (2)$$

Using the data in Table 1 for the calculation in (1), we find that γ = 1.6 for the inner core. Bukowinski (1977) found γ = 1.87, Stacey (1977) found γ = 1.2, and Jamieson, et al. (1978) found γ = 1.5.

Equation (1) is appropriate for insulators. For metals, an electronic contribution must be added. The detailed calculation can be found in Stacey (1977) or in Jamieson, et al. (1978), but as shown by them, adding a small term to γ suffices in place of the detailed calculation because of the smallness of the electronic contribution relative to the lattice term. Following Jamieson, et al., (1977), we will assume that adding 0.1 to γ suffices for the electronic correction. Thus, we shall use

$$\gamma = 1.7 \qquad (3)$$

for the inner core.

We found that the temperature at the Earth's center is 6500° K ± 500. Using the formula developed in lecture 1, Eq. (38)

$$P_{TH} = \frac{\gamma \rho}{(M/V)} R T \qquad (4)$$

we find, P_{TH} = 61 ± 5 GPa at the center.

The temperature is about 300° less at the inner-outer core boundary than in the center, so a good average value for the core is only slightly less at the inner-outer core boundary, and a reasonable value is

$$P_{TH} = 60 \pm 5 \text{ GPa}$$

Table 2. Pressures in the Inner Core Corrected to Absolute Zero

Radius Km	Depth Km	Pressure GPa	Pressure - PREM Corrected to 0° K GPa
0	6371	363.9	299-309
100	6271	363.6	299-309
200	6171	362.9	298-308
300	6071	361.7	297-307
400	5971	360.0	296-306
500	5871	357.9	294-304
600	5771	355.3	291-301
700	5671	352.2	288-298
800	5571	348.7	284-294
900	5471	344.6	280-290
1000	5371	340.2	275-285
1100	5271	335.4	271-281
1200	5171	330.0	265-275
1221.5	5149	328.9	264-274

B. Density Calculations for ε-Iron at Inner Core Pressures.

We can use the last column of Table 2 to test the various isothermal EOS. We need values of ρ_o, K_o, and K_o' at absolute zero. We have found that ε-iron is the phase dominant at

core conditions, and from Table 3, Lecture 3, we have the following at 300° K: $\rho_o = 8.28$, $K_o = 178$, and $K_o' = 5.15$. Now correcting these values to absolute zero, it is found that $\rho_o = 8.29$, $K_o = 180\text{-}186$ GPa and $K_o' = 5.2$. The value of K_o' is weakly constrained from the experiments. This is seen by the two values of α-iron ($K_o' = 5.29$, Guinen and Beshers (1968) and $K_o' = 5.97$, Rotter and Smith (1966)). However, there is no use trying to constrain K_o' better because, as we shall see, there is a trade off between K_o'' and K_o'', which is completely unmeasured.

In order to compute the density at the inner core pressure, we must choose an equation of state. A more fundamental approach for finding the EOS by the quantum mechanics method, such as done by Bukowinski (1977) for γ-iron, has not been made for ε-iron.

It is sufficient here to show that several well known semi-empirical EOS fit the data. We will use several EOS that have been used by various authors in the past to estimate properties of iron at high P. They are the Birch-Murnaghan EOS, the Born-Meyer (method of potentials) EOS, the Morse EOS, the Born-Mie EOS and the Stacey-Irvine EOS. These EOS are not entirely empirical, nor are they used here as curve fitting devices with floating values of the parameters. Instead, we use the three parameters ρ_o, K_o, K_o', determined by experiment in order to determine the resulting trajectory of ρ vs P for the EOS.

The various EOS are listed below (Stacey, et al., 1981):

Birch-Murnaghan (third order)

$$P = \frac{3}{2} K_0 \left((\rho/\rho_0)^{7/3} - (\rho/\rho_0)^{5/3} \right) \left\{ 1 + \frac{3}{4} [K_0' - 4] \left((\rho/\rho_0)^{2/3} - 1 \right) \right\} \tag{6}$$

Birch-Murnaghan (fourth order)

$$P = \frac{3}{2} K_0 \left((\rho/\rho_0)^{7/3} - (\rho/\rho_0)^{5/3} \right) \left\{ 1 + \frac{3}{4} [K_0' - 4] \left((\rho/\rho_0)^{2/3} - 1 \right) + \frac{3}{8} \left(K_0 K_0'' + (K_0' - 4)(K_0' - 3) + \frac{35}{9} \right) \left((\rho/\rho_0)^{2/3} - 1 \right)^2 \right\} + \ldots \tag{7}$$

Morse

$$P = \frac{3K_0}{f} (\rho/\rho_0)^{2/3} \left\{ \exp \left[2f \left(1 - (\rho/\rho_0)^{-1/3} \right) \right] - \exp \left[f \left(1 - (\rho/\rho_0)^{-1/3} \right) \right] \right\}$$

$$f = K_0' - 1, \text{ and } K_0 K_0'' = -1/9 \, (2f^2 + 9f + 2) = -1/9 \, (2K_0'^2 + 5K_0' - 5) \tag{8}$$

$K_0 K_0''$ predetermined by the value of K_0'.

Born-Meyer (method of potentials)

$$P = P(\chi, 0) = 3K_0/(f - 2) \left[\chi^{-2/3} \exp (f - f\chi^{1/3}) - \chi^{-4/3} \right] \tag{9}$$

$$f = 3/2\,(K_0' - 1) + 1/2\left[(3K_0' - 7)^2 + 8\right]^{1/2} \qquad (10)$$

K K_o'' predetermined by value of K_o'.

Born-Mie

$$P = 3K_0/(3K_0' - 8)\left[\chi^{-(K_0'-4/3)} - \chi^{-4/3}\right] \qquad (11)$$

$$K_0K_0'' = -1/3(K_0' - 1) \qquad (12)$$

K K_o'' predetermined by value of K_o'.

Stacey-Irvine

$$P = \frac{K_0}{2\gamma_0}\left(\frac{\rho}{\rho_0}\right)^{+/3}\left\{\exp\left[2\gamma_0\left(1 - \frac{\rho_0}{\rho}\right)\right] - 1\right\} \qquad (13)$$

K_oK_o'' predetermined by value of K_o'.

The use of the Morse equation for compressed iron has been recommended by a number of authors (for example, Boschi, et al., 1979) because of its appropriateness for the metals.

The Born-Meyer (called the Method of Potentials by many Soviet writers) has been used by scientists in the Institute of Physics of the Earth, with good results (Zharkov and Kalinin, 1971).

The Born-Mie is perhaps the simplest third order equation of state giving useful results at very high pressure (Anderson, 1970).

The Stacey-Brennan EOS has a rigorous thermodynamic basis (Brennan and Stacey (1979), and has been applied to iron (Spiliopoulos and Stacey, 1984).

The Birch-Murnaghan EOS is widely used among geoscientists. It also has an empirical advantage: $K_o K_o''$ can be defined independently of K_o'.

The values of P vs ρ are computed for ε-iron for the five EOS listed above, where the zero-temperature values of the parameters (as determined by measurements) are $\rho_o = 8.29$; $K_o^o = 180$, $K_o' = 5.2$. The results are plotted in Figure 1. Here the third order EOS for the Birch-Murnaghan EOS is used. It is concluded that all five EOS come reasonably close to the density profile of the inner core (as corrected to ^oK).

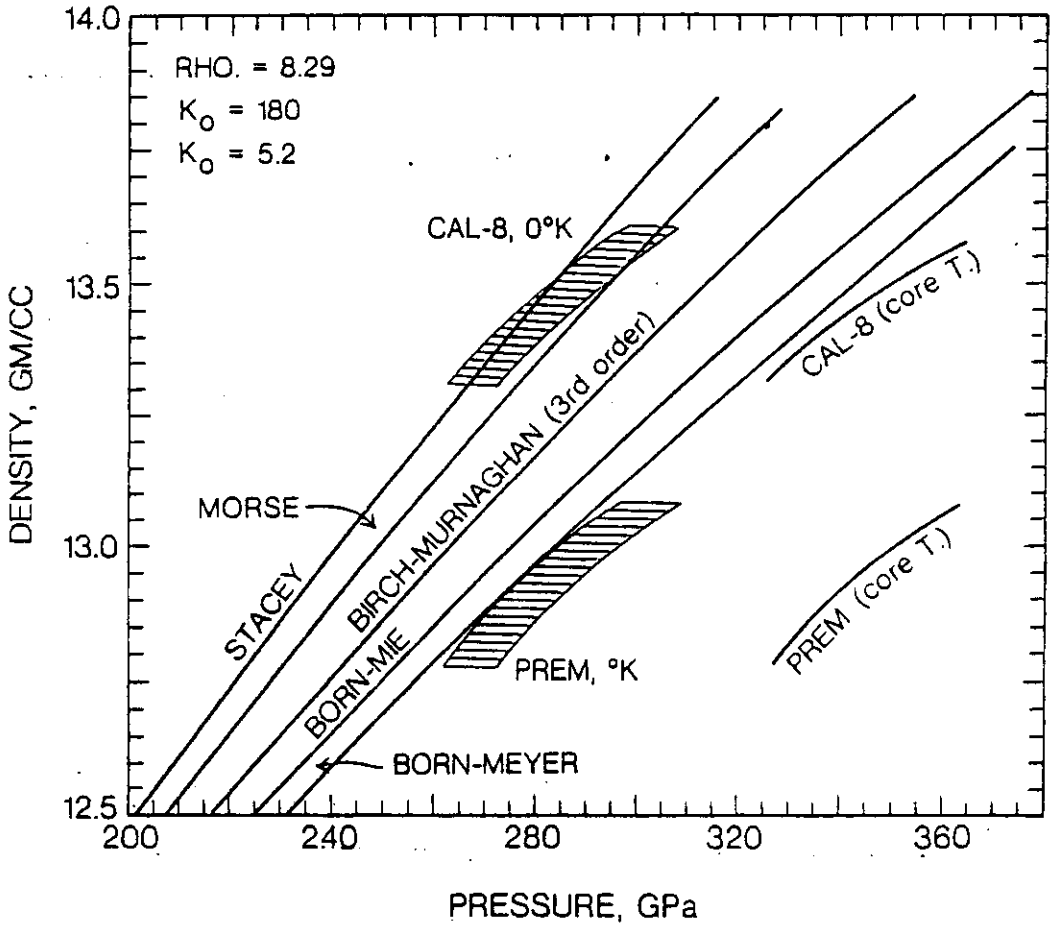

Figure 1. Trajectories of five third order equations of state to inner core pressures, using the zero-temperature value of ρ_o, K_o and K_o determined experimentally. These trajectories are compared with the seismic data of density and pressure (corrected to absolute zero) of two Earth models.

Adjustments in the values of K_o' allowed by the experiments would change the extrapolations, so that any one of the five EOS could be made to intercept either the CAL-8 data or the PREM data. The uncertainty in the measured density of the core is evidenced by the two data sets (PREM and CAL-8).

A fourth order EOS is preferable at these high compressions, so the Birch-Murnaghan EOS is useful for demonstrating the sensitiveness of the extrapolations to the physical parameters of the EOS.

In the third order EOS, $C_4 = 0$, which is obtained from (7) when

$$K_o K_o'' + (K_o' - 4)(K_o' - 3) + 35/9 = 0$$

That is: $C_4 = 0$ for a value of $K_o' = 5.2$, when $K_o K_o'' = -6.53$. Let us allow $K_o K_o''$ to be arbitrary, and map the pairs of values in K_o' and $K_o K_o''$ that makes the Birch-Murnaghan EOS fit either the PREM data or the CAL-8 data.

The resulting values are plotted in Figure 2. Here it is seen that by choosing very reasonable values of K_o' and $K_o K_o''$, the Birch-Murnaghan EOS trajectory can be made to exactly agree with either the PREM data or the Cal-6 data. The shift in the solutions, caused by a higher value of K_o' (186 GPa instead of 180 GPa), is also plotted.

Since the required values of $K_o K_o'$ and K_o are within 10

the bounds of experimental uncertainty, we conclude that ε-iron gives values of density at inner-core conditions in harmony with seismic data of the inner core.

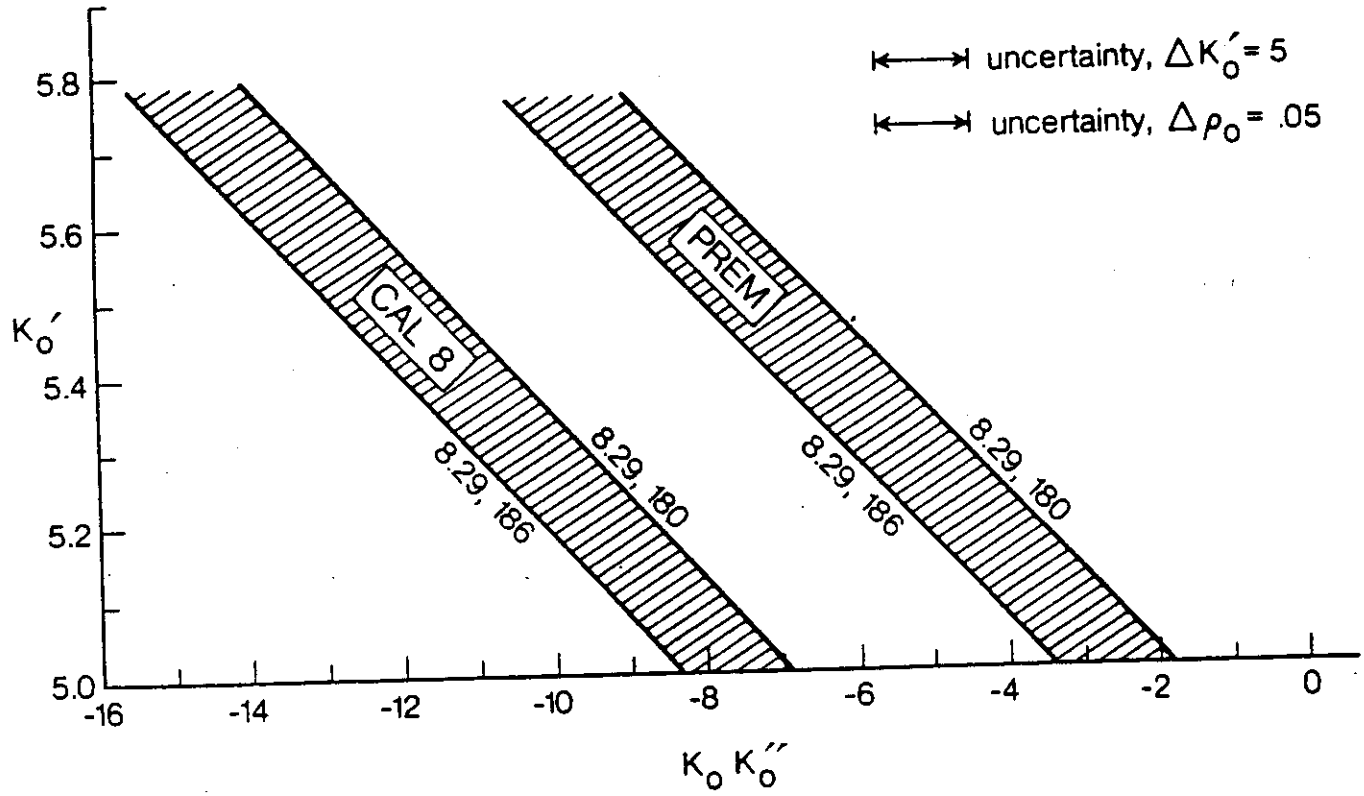

Figure 2. Values of K_o' and $K_o K_o''$ required to make the trajectory of the fourth order Birch-Murnaghan EOS intersect with the pressure density of two seismic models (corrected to absolute zero).

In summary, we find that the choice of ε-iron for the inner core indicated by the shock-wave data is consistent with our present knowledge of the seismic data of the inner core.

References

Anderson, O.L., Elastic constants of the central force model for three cubic structures: Pressure derivatives and equations of state, J. Geophys. Res., 75, 2719-2740, 1970.

Birch, F., The effect of pressure in the elastic properties of isotropic solids according to Murnaghan's theory of finite strain, J. App. Phys., 9, 773, 1938.

Birch, F., Elasticity and composition of the Earth's interior, JGR, 57, 227-286, 1952.

Bolt, B.A., Inside the Earth, Table 4, San Francisco: W.H. Freeman and Co., 1982.

Boschi, E., D. Fazio and F. Mulargia, Theoretical equations of state of iron at the Earth's core conditions, in High Pressure Science and Technology, Vol. (2), edited by K.D. Timmerhaus and M.S. Barber, Plenum Publishing, New York, 1979.

Brennan, B.J. and F. Stacey, A thermodynamically based equation of state for the lower mantle, J. Geophys. Res., 84, 5535-5539, 1979.

Bukowinski, M., A theoretical equation of state for the inner core, Phys. Earth Planet. Inter., 14, 333-43, 1977.

Dziewonski, A.M. and D.L. Anderson, Preliminary reference Earth model, Phys. Earth Planet. Inter., 25, 297-356, 1981.

Guinen, M.W. and Beshers, D.N., Pressure derivatives of the elastic constants of α-iron to 10 KBS, J. Phys. Chem. Solids, 29, 541-549.

Jamieson, J., H.H. Demarest, D. Schiterl, A reevaluation of the Grüneisen parameter for the Earth's core, J. Geophys. Res., 83, 5929, 1978.

Jordan, T.H. and Anderson, D.L., Earth structure from free oscillations and travel times, Geophys. J. R. Astron. Soc., 36, 411-419, 1974.

Morse, P.M., Diatomic molecules according to wave mechanics, II: Vibrational levels, Phys. Rev., 34, 57-64, 1929.

Rotter, C.A. and C.S. Smith, Ultrasonic equation of state of iron, 1. low pressure, room temperature, J. Phys. Chem. Solids, 27, 267-276, 1966.

Spiliopoulos, S. and F.D. Stacey, The Earth's thermal profile: Is there a mid-mantle thermal boundary layer, J. of Geodynamics, 1, 61-77, 1984.

Stacey, F. J., A thermal model of the Earth, PEPI, 15, 341-348, 1957 or 1977?.

Stacey, F.D., B.J. Brennan and R.D. Irvine, Finite strain theories and comparisons with seismological data, Geophys. Surveys, 4, 189-232, 1981.

Zharkov, V. N. and V.A. Kalinin, Equations of state for solids at high pressure and temperature, translated from Russian by A. Tybulewicz, Consultants Bureau, New York, 1971.